

# ROC curve analysis for functional markers

Ana M. Bianco<sup>a</sup>, Graciela Boente<sup>b</sup> and Juan Carlos Pardo-Fernández<sup>c</sup>

<sup>a</sup> Instituto de Cálculo,

Facultad de Ciencias Exactas y Naturales, Universidad de Buenos Aires and CONICET, Argentina

<sup>b</sup> Departamento de Matemáticas and Instituto de Cálculo,

Facultad de Ciencias Exactas y Naturales, Universidad de Buenos Aires and CONICET, Argentina

<sup>c</sup> Centro de Investigación e Tecnoloxía Matemática de Galicia (CITMAga), Universidade de Vigo, Spain

## Abstract

Functional markers become a more frequent tool in medical diagnosis. In this paper, we aim to define an index allowing to discriminate between populations when the observations are functional data belonging to a Hilbert space. We discuss some of the problems arising when estimating optimal directions defined to maximize the area under the curve of a projection index and we construct the corresponding ROC curve. We also go one step forward and consider the case of possibly different covariance operators, for which we recommend a quadratic discrimination rule. Consistency results are derived for both linear and quadratic indexes, under mild conditions. The results of our numerical experiments allow to see the advantages of the quadratic rule when the populations have different covariance operators. We also illustrate the considered methods on a real data set.

## 1 Introduction

In applied sciences, there is a permanent search for better and better tools of diagnosis and screening of different diseases. A key-point is the evaluation of the performance of such developments. The Receiver Operating Characteristic curve (ROC curve) is a very well-accepted

graphical technique to assess the accuracy of a diagnostic test based on a continuous marker. The use of ROC curves is extensive in medical and pharmacological investigations, but they are also employed in completely different scenarios, such as for the evaluation of a machine learning process, see [Krzanowski and Hand \(2009\)](#) where more applications can be found.

For the sole purpose of describing proposals related to the estimation of the ROC curve, we will focus on medical diagnosis, where there are two groups, corresponding to diseased and healthy populations, and the aim is to classify a new subject in one of these groups according to the outcome of a continuous biomarker. In this context, two essential concepts appear concerning the errors one can make: the *sensitivity*, related to the ability of correctly detecting diseased people and the *specificity*, that involves the skill of correctly assigning a subject to the healthy group. Thus, a ROC curve for a test based on a continuous marker is a graphical representation of the *sensitivity* against the complementary of the *specificity* (that is,  $1 - \text{specificity}$ ) computed from the classification rule that assigns a subject to the diseased group if the biomarker is greater than a critical value  $c$  and to the healthy group, otherwise, as the threshold  $c$  varies.

In order to compact the information about the discriminatory performance of the diagnostic test several summary indexes were introduced. The classification accuracy is frequently measured through the area under the curve (AUC), which can be interpreted as the average sensitivity for all specificity values. The Youden index, YI, is another global measure that is extensively used in the literature and is the maximum difference between the ROC curve and the identity function. Estimation and inference methods regarding ROC curve and related summary measures are very well-studied in the univariate setting. [Pepe \(2003\)](#) and [Zhou et al. \(2011\)](#) provide a comprehensive review concerning both theoretical and practical aspects of ROC curves based on univariate markers.

For some diseases, it is necessary to combine several biomarkers in order to get a diagnosis tool that improves the performance of each single marker on its own. In such cases, a global diagnostic measure is desirable to achieve a better classification rule. [Pérez-Fernández \(2020\)](#) reviews some proposals given to summarize the joint information provided by several biomarkers, including methods based on linear and quadratic discrimination rules.

In recent years with the evolution of biomedical technology, data with more and more

complex structure are collected. This is the case of functional data that consist of curves varying over time or any other continuum and thus, valued in an infinite-dimensional space, usually a metric or semi-metric, and in some cases, a Hilbert space. Henceforth, we will assume that the functional data are measured over time. In fact, functional markers have been increasingly used in clinical studies to diagnose diseases. To summarize the curves in a univariate biomarker usual practices are to consider the maximum or minimum values, the time to the maximum or the integral of the curve over the time range. However, specifically designed techniques should be employed to analyse this kind of data in order to take advantage of their potential and, as extensively discussed, the infinite-dimensional structure should be taken into account when considering any estimation procedure, see [Wang et al. \(2016\)](#). For an overview on functional data analysis we refer among others to [Ramsay and Silverman \(2005\)](#), [Ferraty and Vieu \(2006\)](#), [Horváth and Kokoszka \(2012\)](#) and [Hsing and Eubank \(2015\)](#).

Our contribution is oriented to situations such as the one described in Section 6, where we address a study on breast cancer patients with high levels of the protein human epidermal growth factor receptor 2 (HER2). These patients have a better response to drugs that target the HER2 protein, but this kind of therapies may have side effects such as cardiotoxicity. In order to prevent therapy-related cardiac dysfunction (CTRCD), it is recommended to follow-up the appearance of CTRCD through cardiac imaging tests such as the Tissue Doppler Imaging (TDI), an echocardiographic technique that reflects the myocardial motion. TDI is processed so as to obtain a functional datum used to study the heart status. The aim is to evaluate the performance of this functional biomarker, which is displayed in Figure 1, to distinguish between patients with CTRCD from those who do not suffer from this condition.

Functional data, that become more frequent every day in clinical research, pose different challenges to Statistics, in particular, to ROC curve estimation. In this direction, some developments were done to extend the existing methodology to the functional setting. For instance, proposals for the induced ROC considering a univariate marker and a functional covariate are considered by [Inácio et al. \(2012\)](#) and [Inácio de Carvalho et al. \(2016\)](#). However, in some situations, the biomarker itself is a functional data usually discretely recorded. This is usually the case in longitudinal studies and we refer to [Liu and Wu \(2003\)](#) and [Liu et al. \(2005\)](#), who propose a generalized mixed model to predict the condition (healthy or diseased) based on the

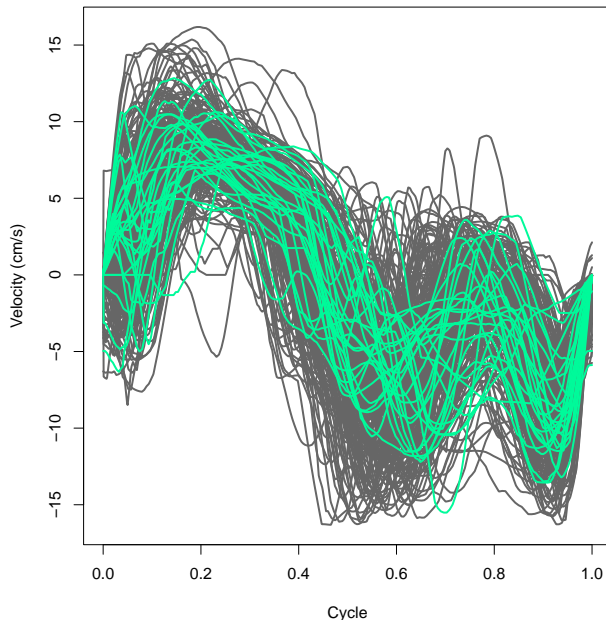


Figure 1: Cardiotoxicity data. Cycles of 270 patients during the follow-up. The cycles of patients with CTRCD= 0 are displayed as gray lines, while those with CTRCD= 1 are represented in aquamarine.

observed values of the biomarker. [Haben et al. \(2019\)](#) consider a dynamic scoring prediction rule and then, several extensions of the ROC curve are introduced. When the biomarker is discretely recorded with some possible noise, smoothing techniques, such as smoothing splines and kernel smoothing, can be employed, see [Wang et al. \(2016\)](#).

[Jang and Mantunga \(2022\)](#) consider a wide class of features to summarize the functional biomarker, including an integral-type that can also be viewed as the inner  $L^2$ -product between the functional data and the constant function that corresponds to the average value of the functional marker. The average velocity and average acceleration as well as the maximum and minimum of the biomarker curve are also considered among these features. The ROC curves and the corresponding AUC are then constructed using the summary functional and the smoothed trajectories.

[Estévez-Pérez and Vieu \(2021\)](#) define a functional version of the ROC curve by properly ranking the sample of functional data via the projection over a selected subset  $\mathcal{E}$  of the functional space indexed by a real number  $\theta \in [0, 1]$ . The functional ROC curve is then defined as the ROC

of the projections over  $\mathcal{E}$ . As mentioned therein, their proposal is appropriate when differences between healthy and diseased individuals arise in their mean, but not on the covariances.

In this paper, we follow a different approach. We first review in Section 2 the basic notions related to ROC curves and the situation of multivariate biomarkers, where methods based on searching for linear combinations maximizing the AUC were given. We consider, in particular, the binormal setting. Later on, in Section 3 we adapt these revisited ideas to the functional framework assuming that the trajectories belong to a Hilbert space and we discuss the issues involved in the estimation of the optimal directions. We also go one step forward, by considering the case of possibly different covariance operators. Section 4 is devoted to the study of asymptotic properties, such as the uniform consistency of the proposed ROC estimators and the strong consistency of the related estimators of the AUC and the Youden index. In Section 5 a thorough numerical experiment is performed, while the analysis of the real data set mentioned above illustrates the application of the studied procedures in Section 6. Some final comments are provided in Section 7. Proofs are relegated to the Appendix.

## 2 Preliminaries

### 2.1 Basic notions and multivariate biomarkers

We begin by introducing basic concepts related to ROC curves in the simple case of a univariate biomarker. Assume that  $Y$  is a continuous biomarker and let  $c$  be a threshold value. Thus, we consider the classification rule that assigns a subject to the diseased group when  $Y \geq c$  and to the healthy population, otherwise. Moreover, denote  $Y_D$  the marker in the diseased population and  $F_D$  its distribution, while  $Y_H$  and  $F_H$  stand for the marker and its distribution in the healthy population. Our interest focuses on the evolution of the pairs  $\{(1 - F_H(c), 1 - F_D(c))\}$  as  $c \in \mathbb{R}$  varies. This leads to the usual ROC curve formula given by  $\text{ROC}(p) = 1 - F_D(F_H^{-1}(1 - p))$ ,  $p \in (0, 1)$ .

An extensively used model is the binormal one, that assumes that in both independent populations the marker is normally distributed, i.e.,  $F_j \sim N(\mu_j, \sigma_j)$ , for  $j = D, H$ . In this case, the distributions are characterized by the means  $\mu_j$  and the standard deviations  $\sigma_j$ ,  $j = D, H$ ,

leading to  $\text{ROC}(p) = \Phi((\mu_H - \mu_D)/\sigma_D + \sigma_H\Phi^{-1}(p)/\sigma_D)$ , where  $\Phi$  stands for the cumulative distribution function of a standard normal.

In order to have a global measure of the accuracy of the test, different indexes have been introduced. The area under the ROC curve (AUC) is the most popular and is defined as  $\text{AUC} = \int_0^1 \text{ROC}(p)dp$ . Straightforward calculus enables to prove that  $\text{AUC} = \mathbb{P}(Y_D > Y_H)$  and this is why values of AUC near to 1 are related to high diagnostic accuracy of the biomarker. The Youden index, YI, is also very well known. It measures the proximity of the ROC curve to the identity function, thinking of the identity as the ROC of useless marker and is defined as  $\text{YI} = \max_{0 < p < 1} \{\text{ROC}(p) - p\}$ . It is worth mentioning that when  $Y_D$  is stochastically greater than  $Y_H$ , then  $\text{ROC}(p) \geq p$ , so the area under the curve is greater or equal than 0.5 and the Youden index is non-negative.

Now, let us consider the multivariate case where  $\mathbf{x} \in \mathbb{R}^k$  the multivariate biomarker is used for the diagnostic of a given disease. From now on,  $\mathbf{x}_D \sim F_D$  and  $\mathbf{x}_H \sim F_H$  stand for the independent biomarkers over the diseased and healthy populations, respectively. A well known discrimination rule is the linear one, which intends to project the data over a given direction chosen to differentiate both groups. For a given  $\boldsymbol{\beta} \in \mathbb{R}^k$  denote  $Y_{j,\boldsymbol{\beta}} = \boldsymbol{\beta}^T \mathbf{x}_j$ , for  $j = D, H$ , and let  $F_{j,\boldsymbol{\beta}}$  their respective distribution functions. Then, a ROC curve can be constructed for each fixed  $\boldsymbol{\beta} \neq \mathbf{0}_k$  as

$$\text{ROC}_{\boldsymbol{\beta}}(p) = 1 - F_{D,\boldsymbol{\beta}}(F_{H,\boldsymbol{\beta}}^{-1}(1-p)), \quad p \in (0, 1).$$

$\text{ROC}_{\boldsymbol{\beta}}$  allows to evaluate the capability of the projected biomarker to distinguish between the two groups. Among others, [Ma and Huang \(2005\)](#) and [Pepe et al. \(2006\)](#) provide methods to choose the best direction by means of the area under the curve  $\text{AUC}(\boldsymbol{\beta}) = \int_0^1 \text{ROC}_{\boldsymbol{\beta}}(p)dp = \mathbb{P}(Y_{D,\boldsymbol{\beta}} > Y_{H,\boldsymbol{\beta}})$ . In [Section 2.2](#), we review the construction of the optimal direction on a population level for normally distributed biomarkers, to understand how these ideas extend to the functional case, as presented in [Section 3.1](#).

## 2.2 Binormal case

The binormal model has been extensively considered for univariate biomarkers as a way to supply a simple parametric approach to ROC curves estimation. Hence, if the practitioner

suspects that this model gives a suitable approximation, they can choose the threshold constants according to that belief, providing a semiparametric framework that will indeed keep consistency under the suspected model. In the multivariate setting, the binormal model also provides a simple expression for both the  $\text{ROC}_\beta(p)$  and the  $\text{AUC}(\beta)$ .

Let us assume that  $\mathbf{x}_j \sim N(\boldsymbol{\mu}_j, \boldsymbol{\Sigma}_j)$ , hence  $Y_{j,\beta} \sim N(\boldsymbol{\beta}^\top \boldsymbol{\mu}_j, \boldsymbol{\beta}^\top \boldsymbol{\Sigma}_j \boldsymbol{\beta})$ . Denote  $z_p$  the value such that  $\Phi(z_p) = 1 - p$ . As it is well known, in such framework, the quantile and distribution functions of  $Y_{H,\beta}$  and  $Y_{D,\beta}$ , respectively have an explicit expression given by

$$F_{H,\beta}^{-1}(1-p) = \boldsymbol{\beta}^\top \boldsymbol{\mu}_H + \sqrt{\boldsymbol{\beta}^\top \boldsymbol{\Sigma}_H \boldsymbol{\beta}} z_p \quad \text{and} \quad F_{D,\beta}(u) = \Phi\left(\frac{u - \boldsymbol{\beta}^\top \boldsymbol{\mu}_D}{\sqrt{\boldsymbol{\beta}^\top \boldsymbol{\Sigma}_D \boldsymbol{\beta}}}\right),$$

which allow to express the related  $\text{ROC}_\beta$  curve using the cumulative standard normal distribution as

$$\text{ROC}_\beta(p) = 1 - F_{D,\beta}\left(\boldsymbol{\beta}^\top \boldsymbol{\mu}_H + \sqrt{\boldsymbol{\beta}^\top \boldsymbol{\Sigma}_H \boldsymbol{\beta}} z_p\right) = 1 - \Phi\left(\frac{\boldsymbol{\beta}^\top (\boldsymbol{\mu}_H - \boldsymbol{\mu}_D) + \sqrt{\boldsymbol{\beta}^\top \boldsymbol{\Sigma}_H \boldsymbol{\beta}} z_p}{\sqrt{\boldsymbol{\beta}^\top \boldsymbol{\Sigma}_D \boldsymbol{\beta}}}\right).$$

Furthermore, taking into account that  $Y_{D,\beta} - Y_{H,\beta} \sim N(\boldsymbol{\beta}^\top (\boldsymbol{\mu}_D - \boldsymbol{\mu}_H), \boldsymbol{\beta}^\top (\boldsymbol{\Sigma}_D + \boldsymbol{\Sigma}_H) \boldsymbol{\beta})$ , an explicit expression may also be given for the  $\text{AUC}(\beta)$  as

$$\text{AUC}(\beta) = \mathbb{P}(Y_{D,\beta} - Y_{H,\beta} > 0) = \Phi\left(\frac{\boldsymbol{\beta}^\top (\boldsymbol{\mu}_D - \boldsymbol{\mu}_H)}{[\boldsymbol{\beta}^\top (\boldsymbol{\Sigma}_D + \boldsymbol{\Sigma}_H) \boldsymbol{\beta}]^{\frac{1}{2}}}\right).$$

Ma and Huang (2007) propose to estimate  $\beta$  as the value maximizing a smooth estimator,  $\widehat{\text{AUC}}(\beta)$ , of  $\text{AUC}(\beta)$ . Taking into account that the area under the curve and  $\text{ROC}_\beta$  remain unchanged if  $\beta$  is multiplied by a positive constant, Ma and Huang (2007) suggest to maximize  $\widehat{\text{AUC}}(\beta)$  over the values  $\beta$  such that the first coordinate equals 1. When constructing the smooth estimator  $\widehat{\text{AUC}}(\beta)$  the indicator function is approximated by the sigmoid function.

It is clear that the population counterparts of the estimators defined in Ma and Huang (2007) correspond to the value  $\beta$  maximizing  $\text{AUC}(\beta)$  over the directions with its first component equal to 1, or equivalently to the maximizer of

$$L(\beta) = \frac{\boldsymbol{\beta}^\top (\boldsymbol{\mu}_D - \boldsymbol{\mu}_H)}{[\boldsymbol{\beta}^\top (\boldsymbol{\Sigma}_D + \boldsymbol{\Sigma}_H) \boldsymbol{\beta}]^{\frac{1}{2}}}. \quad (1)$$

The Cauchy–Schwartz inequality implies that any scalar multiple of  $\beta_0 = (\boldsymbol{\Sigma}_D + \boldsymbol{\Sigma}_H)^{-1} (\boldsymbol{\mu}_D - \boldsymbol{\mu}_H)$  maximizes  $|L(\beta)|$ , so  $\beta_0$  (and any positive multiple of it) maximizes  $\text{AUC}(\beta)$  leading to

$$\max_{\beta} \text{AUC}(\beta) = \text{AUC}(\beta_0) = \Phi\left([\boldsymbol{\mu}_D - \boldsymbol{\mu}_H]^\top (\boldsymbol{\Sigma}_D + \boldsymbol{\Sigma}_H)^{-1} (\boldsymbol{\mu}_D - \boldsymbol{\mu}_H)\right]^{\frac{1}{2}}.$$

Note that when  $\Sigma_D = \Sigma_H$ , the Fisher discriminating direction is obtained.

Define  $\mathcal{A}_\beta(p) = \{\mathbf{x} \in \mathbb{R}^k : \beta^\top \mathbf{x} \geq \beta^\top \boldsymbol{\mu}_H + \sqrt{\beta^\top \Sigma_H \beta} z_p\}$ , so that  $\mathbb{P}(\mathbf{x}_H \in \mathcal{A}_\beta(p)) = p$ . Then, using that  $\mathbf{x}_D \sim N(\boldsymbol{\mu}_D, \Sigma_D)$  and denoting as  $Z \sim N(0, 1)$ , we get that

$$\begin{aligned} \mathbb{P}(\mathbf{x}_D \in \mathcal{A}_\beta(p)) &= \mathbb{P}\left(\beta^\top \mathbf{x}_D \geq \beta^\top \boldsymbol{\mu}_H + \sqrt{\beta^\top \Sigma_H \beta} z_p\right) \\ &= \mathbb{P}\left(Z \geq \frac{\beta^\top (\boldsymbol{\mu}_H - \boldsymbol{\mu}_D) + \sqrt{\beta^\top \Sigma_H \beta} z_p}{\sqrt{\beta^\top \Sigma_D \beta}}\right) \\ &= 1 - \Phi\left(\frac{\beta^\top (\boldsymbol{\mu}_H - \boldsymbol{\mu}_D) + \sqrt{\beta^\top \Sigma_H \beta} z_p}{\sqrt{\beta^\top \Sigma_D \beta}}\right) \\ &= \Phi\left(\frac{\beta^\top (\boldsymbol{\mu}_D - \boldsymbol{\mu}_H) - \sqrt{\beta^\top \Sigma_H \beta} z_p}{\sqrt{\beta^\top \Sigma_D \beta}}\right), \end{aligned} \quad (2)$$

which implies that  $\text{ROC}_\beta(p) = \mathbb{P}(\mathbf{x}_D \in \mathcal{A}_\beta(p))$ .

From now on, to simplify the discussion below, assume that  $\Sigma_j = \Sigma$ , for  $j = D, H$ .

A global ROC curve has been defined as  $\text{ROC}(p) = \sup_{\|\beta\|=1} \mathbb{P}(\mathbf{x}_D \in \mathcal{A}_\beta(p))$ . Using (2) and that  $\Sigma_j = \Sigma$ , we obtain that the global ROC curve equals

$$\begin{aligned} \text{ROC}(p) &= \sup_{\|\beta\|=1} \left\{ \Phi\left(\frac{\beta^\top (\boldsymbol{\mu}_D - \boldsymbol{\mu}_H) - \sqrt{\beta^\top \Sigma \beta} z_p}{\sqrt{\beta^\top \Sigma \beta}}\right) \right\} \\ &= \sup_{\|\beta\|=1} \left\{ \Phi\left(\frac{\beta^\top (\boldsymbol{\mu}_D - \boldsymbol{\mu}_H)}{\sqrt{\beta^\top \Sigma \beta}} - z_p\right) \right\} = \sup_{\|\beta\|=1} \left\{ \Phi\left(\sqrt{2} L(\beta) - z_p\right) \right\}. \end{aligned}$$

Hence, taking into account that  $\beta_0$  maximizes  $L(\beta)$ , we obtain that the supremum is a maximum and is attained at  $\beta_0 = \Sigma^{-1} (\boldsymbol{\mu}_D - \boldsymbol{\mu}_H)$ . Therefore, the global ROC is given by

$$\begin{aligned} \text{ROC}(p) &= \text{ROC}_{\beta_0}(p) = \Phi\left(\sqrt{(\boldsymbol{\mu}_D - \boldsymbol{\mu}_H)^\top \Sigma^{-1} (\boldsymbol{\mu}_D - \boldsymbol{\mu}_H)} - z_p\right) \\ &= 1 - \Phi\left(z_p - \sqrt{(\boldsymbol{\mu}_D - \boldsymbol{\mu}_H)^\top \Sigma^{-1} (\boldsymbol{\mu}_D - \boldsymbol{\mu}_H)}\right), \end{aligned}$$

meaning that the global ROC curve is the ROC curve associated to the optimal direction with respect to the area under the curve.

Beyond the AUC, the Youden index, which as explained above measures the difference between the ROC curve and the identity function, may also be maximized to obtain the associated optimal direction. In this case, the induced optimality problem searches for the direction  $\beta$  such that

$$\text{YI}(\beta) = \max_{c \in \mathbb{R}} \left| \Phi\left(\frac{c - \beta^\top \boldsymbol{\mu}_D}{\sqrt{\beta^\top \Sigma \beta}}\right) - \Phi\left(\frac{c - \beta^\top \boldsymbol{\mu}_H}{\sqrt{\beta^\top \Sigma \beta}}\right) \right| = \max_{c \in \mathbb{R}} \Delta_\beta(c)$$



is maximum. Straightforward calculations relegated to the Appendix allow to show that

$$\operatorname{argmax}_{\|\boldsymbol{\beta}\|=1} \text{YI}(\boldsymbol{\beta}) = \frac{\boldsymbol{\Sigma}^{-1}(\boldsymbol{\mu}_D - \boldsymbol{\mu}_H)}{\sqrt{(\boldsymbol{\mu}_D - \boldsymbol{\mu}_H)^T \boldsymbol{\Sigma}^{-1}(\boldsymbol{\mu}_D - \boldsymbol{\mu}_H)}}. \quad (3)$$

Hence, if the covariance matrices are equal, the value  $\boldsymbol{\beta}$  maximizing  $\text{YI}(\boldsymbol{\beta})$  is proportional to  $\boldsymbol{\Sigma}^{-1}(\boldsymbol{\mu}_D - \boldsymbol{\mu}_H)$  and all summary measures lead to the same optimal value.

### 3 Functional setting

In this section, we consider functional biomarkers belonging to a separable Hilbert space. More precisely, we assume that  $X_j \in \mathcal{H} = L^2(0,1)$ ,  $j = D, H$ , and denote as  $P_j$  the probability measure related to  $X_j$ . From now on,  $\|\cdot\|$  and  $\langle \cdot, \cdot \rangle$  stand for the norm and the inner product in  $\mathcal{H}$ .

Let  $\Upsilon : \mathcal{H} \rightarrow \mathbb{R}$  an operator used as discrimination index to classify a new observation to one of the two classes. Clearly, from this index a related ROC may be defined as

$$\text{ROC}_\Upsilon(p) = 1 - F_{\Upsilon,D}(F_{\Upsilon,H}^{-1}(1-p)), \quad p \in (0,1), \quad (4)$$

where  $F_{\Upsilon,D}$  and  $F_{\Upsilon,H}^{-1}$  stand for the distribution function and quantile function of  $Y_{\Upsilon,j} = \Upsilon(X_j)$ ,  $j = D, H$ , respectively, that is,  $F_{\Upsilon,j}(u) = P_j(\Upsilon(X_j) \leq u)$ . The related area under the curve is then obtained as

$$\text{AUC}_\Upsilon = \mathbb{P}(Y_{\Upsilon,D} > Y_{\Upsilon,H}).$$

When independent samples  $X_{j,i}$ ,  $1 \leq i \leq n_j$ ,  $j = D, H$ , are available, estimators of  $\text{ROC}_\Upsilon$  and  $\text{AUC}_\Upsilon$  may be obtained if the discriminating index has a closed form, as it is the case for integral of the biomarker curve, its maximum and/or minimum and other features described in [Jang and Mantunga \(2022\)](#). In this case, defining,  $Y_{j,i} = \Upsilon(X_{j,i})$ ,  $1 \leq i \leq n_j$ ,  $j = D, H$ , the ROC estimator is obtained as

$$\widehat{\text{ROC}}(p) = \widehat{\text{ROC}}_\Upsilon(p) = 1 - \widehat{F}_{\Upsilon,D}(F_{\Upsilon,H}^{-1}(1-p)), \quad p \in (0,1), \quad (5)$$

where  $\widehat{F}_{\Upsilon,D}$  and  $\widehat{F}_{\Upsilon,H}^{-1}$  stand for the empirical distribution function and quantile function of the samples  $Y_{j,i}$ ,  $1 \leq i \leq n_j$ ,  $j = D, H$ , respectively. From the univariate index, the AUC estimator is defined as

$$\widehat{\text{AUC}} = \widehat{\text{AUC}}_\Upsilon = \frac{1}{n_D n_H} \sum_{i=1}^{n_D} \sum_{\ell=1}^{n_H} \mathbb{I}_{\{Y_{D,i} > Y_{H,\ell}\}}.$$

In some situations as those defined below, the index depends on unknown parameters and needs to be predicted. Denote  $\widehat{\Upsilon}$  the predicted discrimination index, and as  $\widehat{Y}_{j,i} = \widehat{\Upsilon}(X_{j,i})$ ,  $1 \leq i \leq n_j$ ,  $j = D, H$ . Then, the ROC and AUC estimators may be defined as

$$\widehat{\text{ROC}}(p) = \widehat{\text{ROC}}_{\widehat{\Upsilon}}(p) = 1 - \widehat{F}_{\widehat{\Upsilon},D} \left( \widehat{F}_{\widehat{\Upsilon},H}^{-1}(1-p) \right), \quad p \in (0, 1), \quad (6)$$

$$\widehat{\text{AUC}} = \widehat{\text{AUC}}_{\widehat{\Upsilon}} = \frac{1}{n_D n_H} \sum_{i=1}^{n_D} \sum_{\ell=1}^{n_H} \mathbb{I}_{\{\widehat{Y}_{D,i} > \widehat{Y}_{H,\ell}\}}, \quad (7)$$

where  $\widehat{F}_{\widehat{\Upsilon},D}$  and  $\widehat{F}_{\widehat{\Upsilon},D}^{-1}$  stand now for the empirical distribution function and quantile function of the samples  $\widehat{Y}_{j,i} = \widehat{\Upsilon}(X_{j,i})$ ,  $1 \leq i \leq n_j$ ,  $j = D, H$ , respectively.

## 3.1 Linear discriminating index

### 3.1.1 An index that maximizes the AUC

We begin by considering the situation where  $X_j$  are Gaussian processes with mean  $\mu_j$  and covariance operator  $\Gamma_j$ , denoted  $\mathcal{G}(\mu_j, \Gamma_j)$ . Then, if  $\beta \in \mathcal{H}$ ,  $\|\beta\| = 1$ , and we denote  $Y_{j,\beta} = \langle \beta, X_j \rangle$ , for  $j = D, H$ , and by  $F_{j,\beta}$  their distribution functions, we have that  $Y_{j,\beta} \sim N(\langle \beta, \mu_j \rangle, \langle \beta, \Gamma_j \beta \rangle)$  whenever  $\beta \notin \text{Ker}(\Gamma_j)$ . It is worth mentioning that if the kernel of  $\Gamma_j$  does not reduce to 0, for any  $\beta \in \text{Ker}(\Gamma_j)$ , we have that  $\mathbb{P}(Y_{j,\beta} = \langle \beta, \mu_j \rangle) = 1$ . Taking into account that  $\mu_j \in \text{Ker}(\Gamma_j)^\perp$ , we have that, if  $\Gamma_D = \Gamma_H = \Gamma$ ,  $\text{Ker}(\Gamma) \neq \{0\}$  and  $\beta \in \text{Ker}(\Gamma)$ , we have that  $\mathbb{P}(Y_{j,\beta} = 0) = 1$ , for  $j = D, H$ , and the two populations cannot be distinguished in such directions.

As in the multivariate case for each fixed  $\beta \in \mathcal{H}$ ,  $\|\beta\| = 1$ ,  $\beta \notin \text{Ker}(\Gamma_D) \cap \text{Ker}(\Gamma_H)$ , the AUC associated to the new independent biomarkers  $Y_{j,\beta}$  is given by

$$\text{AUC}(\beta) = \mathbb{P}(Y_{D,\beta} > Y_{H,\beta}) = \Phi \left( \frac{\langle \beta, \mu_D - \mu_H \rangle}{[\langle \beta, (\Gamma_H + \Gamma_D) \beta \rangle]^{\frac{1}{2}}} \right).$$

Then, if we denote  $\Gamma_A = (\Gamma_H + \Gamma_D)/2$  the element  $\beta_0$  maximizing  $\text{AUC}(\beta)$  may be obtained up to a positive constant as  $\beta_0 = \text{argmax}_{\beta \neq 0} L(\beta)$ , where

$$L(\beta) = \frac{\langle \beta, \mu_D - \mu_H \rangle}{[2\langle \beta, \Gamma_A \beta \rangle]^{\frac{1}{2}}}. \quad (8)$$

It is worth mentioning the analogy with the expression given in (1).

Unlike the multivariate case and as in canonical correlation, this maximization problem poses some challenges due to the infinite-dimensional structure. The major problem is due

to the fact that the operator  $\Gamma_A = (\Gamma_H + \Gamma_D)/2$  is compact and then it does not have an inverse. To clarify the difficulties and the relation to canonical correlation, let  $X$  be such that  $X|G = 1 \sim X_D$  and  $X|G = 0 \sim X_H$  with  $G$  a binary variable indicating the group membership, such that  $\mathbb{P}(G = 1) = \pi_D$  and denote  $\pi_H = 1 - \pi_D$ .

**Lemma 3.1.** *Let  $L_{\text{POOL}}(\beta)$  be defined as*

$$L_{\text{POOL}}(\beta) = \frac{\langle \beta, \mu_D - \mu_H \rangle}{[2\langle \beta, \Gamma_{\text{POOL}}\beta \rangle]^{\frac{1}{2}}},$$

where  $\Gamma_{\text{POOL}} = \pi_D\Gamma_D + \pi_H\Gamma_H$ . Then,

a) for any  $\beta \notin \text{Ker}(\Gamma_D) \cap \text{Ker}(\Gamma_H)$ ,

$$\text{corr}^2(\langle \beta, X \rangle, G) = \pi_D\pi_H \left( 1 - \frac{1}{1 + L_{\text{POOL}}^2(\beta)} \right).$$

b) When  $\pi_D = 1/2$  or when  $\Gamma_H = \Gamma_D$ , the problem of maximizing the AUC and that of maximizing  $\text{corr}(\langle \beta, X \rangle, G)$  coincide.

In the sequel  $\Gamma$  will denote either  $\Gamma_{\text{POOL}}$  or  $\Gamma_A$ . Note that when  $\Gamma_H = \Gamma_D$ , then  $\Gamma_{\text{POOL}} = \Gamma_A = \Gamma$ . The following proposition provides an explicit expression for the direction maximizing  $L_{\text{POOL}}^2(\beta)$  and/or the AUC.

From now on denote  $\lambda_1 \geq \lambda_2 \geq \dots$  the eigenvalues of  $\Gamma$  and  $\phi_j$  the corresponding eigenfunctions.

**Proposition 3.2.** *Let us assume that the eigenvalues  $\lambda_j$  of  $\Gamma$  are all positive and define the linear space*

$$\mathcal{R}(\Gamma) = \left\{ y \in \mathcal{H} : \sum_{\ell \geq 1} \frac{1}{\lambda_\ell^2} \langle y, \phi_\ell \rangle^2 < \infty \right\},$$

and the inverse of  $\Gamma : \mathcal{R}(\Gamma) \rightarrow \mathcal{H}$  as

$$\Gamma^{-1}(y) = \sum_{\ell \geq 1} \frac{1}{\lambda_\ell} \langle y, \phi_\ell \rangle \phi_\ell, \quad \text{for any } y \in \mathcal{R}(\Gamma).$$

Furthermore, assume that  $\mu_D - \mu_H \in \mathcal{R}(\Gamma)$ . Then, if  $\Gamma = \Gamma_{\text{POOL}}$  and  $\beta_0$  stands for the value maximizing  $L_{\text{POOL}}^2(\beta)$  or if  $\Gamma = \Gamma_A$  and  $\beta_0$  stands for the value maximizing the AUC, then  $\beta_0 = \sqrt{\pi_D\pi_H} \Gamma^{-1}(\mu_D - \mu_H)$ .

**Remark 3.1.** *It is worth mentioning that similar arguments to those considered above allow to show that  $\beta_0$  still maximizes the AUC if the biomarkers have an elliptical distribution, as defined in [Bali and Boente \(2009\)](#) and studied in [Boente et al. \(2014\)](#). In what follows we briefly present the arguments leading to this conclusion.*

To state the definition of elliptical distributions in a functional setting, we will first remind the basic concept of elliptical distributions in  $\mathbb{R}^k$ . Recall that a random vector  $\mathbf{z} \in \mathbb{R}^k$  is said to have a  $k$ -dimensional spherical distribution if its distribution is invariant under orthogonal transformations. In general, the characteristic function of a spherically distributed  $\mathbf{x} \in \mathbb{R}^k$  is of the form  $\psi_{\mathbf{x}}(\mathbf{t}_k) = \varphi(\mathbf{t}_k^T \mathbf{t}_k)$  for  $\mathbf{t}_k \in \mathbb{R}^k$ , and any distribution in  $\mathbb{R}^k$  having a characteristic function of this form is a spherical distribution. Hence, we can denote a spherically distributed vector as  $\mathbf{x} \sim \mathcal{S}_k(\varphi)$ , which is convenient since, for  $\mathbf{x}^T = (\mathbf{x}_1^T, \mathbf{x}_2^T)$  with  $\mathbf{x}_1 \in \mathbb{R}^m$ , we have that  $\mathbf{x}_1 \sim \mathcal{S}_m(\varphi)$ .

Elliptical distributions in  $\mathbb{R}^k$  correspond distributions obtained from affine transformations of spherically distributed random vectors in  $\mathbb{R}^k$ . More precisely, for a given matrix  $\mathbf{A} \in \mathbb{R}^{k \times k}$  and a vector  $\boldsymbol{\mu} \in \mathbb{R}^k$ , the distribution of  $\mathbf{x} = \mathbf{A}\mathbf{z} + \boldsymbol{\mu}$  when  $\mathbf{z} \sim \mathcal{S}_k(\varphi)$  is said to have an elliptical distribution, denoted  $\mathbf{x} \sim \mathcal{E}_k(\boldsymbol{\mu}, \boldsymbol{\Sigma}, \varphi)$ , where  $\boldsymbol{\Sigma} = \mathbf{A}\mathbf{A}^T$ . When first moment exists,  $\mathbb{E}(\mathbf{X}) = \boldsymbol{\mu}$ . Furthermore, when second moments exist then the covariance matrix of  $\mathbf{x}$  is proportional to  $\boldsymbol{\Sigma}$ .

It is easy to see that the characteristic function of  $\mathbf{x}$  equals  $\psi_{\mathbf{x}}(\mathbf{t}) = \exp(i\mathbf{t}^T \boldsymbol{\mu})\varphi(\mathbf{t}^T \boldsymbol{\Sigma} \mathbf{t})$ . Hence, the scatter matrix  $\boldsymbol{\Sigma}$  is confounded with the function  $\varphi$  in the sense that, for any  $c > 0$ ,  $\mathcal{E}_k(\boldsymbol{\mu}, \boldsymbol{\Sigma}, \varphi) \sim \mathcal{E}_k(\boldsymbol{\mu}, c\boldsymbol{\Sigma}, \varphi_c)$  where  $\varphi_c(w) = \varphi(w/c)$ . For that reason, henceforth, we will assume that the characteristic function  $\varphi$  is chosen so that the covariance matrix of  $\mathbf{x}$  equals  $\boldsymbol{\Sigma}$ .

An important property of elliptical distributions, is that the sum of independent elliptical random vectors with the same scatter matrix  $\boldsymbol{\Sigma}$  is elliptical, see [Hult and Lindskog \(2002\)](#) and [Frahm \(2004\)](#). This fact is important in what follows, since it implies that if  $\mathbf{x}_D \sim \mathcal{E}_k(\boldsymbol{\mu}_D, \boldsymbol{\Sigma}, \varphi_D)$  and  $\mathbf{x}_H \sim \mathcal{E}_k(\boldsymbol{\mu}_H, \boldsymbol{\Sigma}, \varphi_H)$  are independent, then  $\mathbf{x}_D - \mathbf{x}_H \sim \mathcal{E}_k(\boldsymbol{\mu}_D - \boldsymbol{\mu}_H, \boldsymbol{\Sigma}, \varphi_D \times \varphi_H)$  and  $\boldsymbol{\beta}^T(\mathbf{x}_D - \mathbf{x}_H) \sim \boldsymbol{\beta}^T(\boldsymbol{\mu}_D - \boldsymbol{\mu}_H) + z\sqrt{\boldsymbol{\beta}^T \boldsymbol{\Sigma} \boldsymbol{\beta}}$ , where the random variable  $z$  has a symmetric distribution  $G_0$  with characteristic function  $\varphi_z(t) = \varphi_D(t^2) \varphi_H(t^2)$ .

[Bali and Boente \(2009\)](#) define elliptical distributed random elements in a separable Hilbert-space  $\mathcal{H}$  as follows. The random element  $X$  is said to have an elliptical distribution  $\mathcal{E}(\boldsymbol{\mu}, \Gamma, \varphi)$  with parameters  $\boldsymbol{\mu} \in \mathcal{H}$  and  $\Gamma : \mathcal{H} \rightarrow \mathcal{H}$  a self-adjoint, positive semi-definite and compact

operator if and only if for any linear and bounded operator  $A : \mathcal{H} \rightarrow \mathbb{R}^k$ , we have that with adjoint operator  $A^*$ , we have that  $AX \sim \mathcal{E}_k(A\mu, A\Gamma A^*, \varphi)$  where  $A^* : \mathbb{R}^k \rightarrow \mathcal{H}$  stands for the adjoint operator of  $A$ . As noted in [Boente et al. \(2014\)](#),  $X \sim \mathcal{E}(\mu, \Gamma, \varphi)$  if and only if  $\langle a, X \rangle \sim \mathcal{E}_1(\langle a, \mu \rangle, \langle a, \Gamma a \rangle, \varphi)$  for all  $a \in \mathcal{H}$ .

The above discussion implies that, if  $X_j \sim \mathcal{E}(\mu_j, \Gamma, \varphi_j)$ , for  $j = D, H$ , then the AUC of the projected biomarkers can be expressed as

$$AUC(\beta) = \mathbb{P}(Y_{D,\beta} > Y_{H,\beta}) = G_0 \left( \frac{\langle \beta, \mu_D - \mu_H \rangle}{[\langle \beta, \Gamma \beta \rangle]^{\frac{1}{2}}} \right),$$

with  $G_0$  a distribution function symmetric around 0, that is,  $G_0(t) = 1 - G_0(-t)$ . Therefore, the value maximizing the AUC is still the one maximizing  $L_{\text{POOL}}(\beta)$  in (3.1) and is given in [Proposition 3.2](#).

### 3.1.2 Estimating the linear projection index

Suppose that independent samples  $X_{j,i}$ ,  $1 \leq i \leq n_j$ ,  $j = D, H$ , are available. As shown by [Leurgans et al. \(1993\)](#) for the case of canonical correlation between two functional random elements, the sample maximum correlation can attain the value 1, for proper directions. The same arises in the present situation, where the sample version of the AUC may lead to values close to 1 for proper directions, meaning that the maximizer of  $\widehat{L}(\beta)$  or equivalently of  $\widehat{AUC}(\beta)$  will not provide relevant information.

As in functional canonical correlation, the problem may be overcome using basis and/or penalizations. More precisely, let  $D\alpha = \alpha''$  and  $\Psi(\alpha) = \|D\alpha\|$ , then we can penalize the denominator in  $L(\beta)$  to define

$$\widehat{L}_\lambda(\beta) = \frac{\langle \beta, \widehat{\mu}_D - \widehat{\mu}_H \rangle}{\left[ \langle \beta, \widehat{\Gamma} \beta \rangle + \lambda \Psi(\beta) \right]^{\frac{1}{2}}}$$

where  $\widehat{\mu}_D$ ,  $\widehat{\mu}_H$  are estimators of  $\mu_D$  and  $\mu_H$  and  $\widehat{\Gamma}$  is an estimator of  $\Gamma_A$ , such as their sample versions. A typical choice for  $\widehat{\mu}_j$  is the sample mean  $\bar{X}_j = (1/n_j) \sum_{i=1}^{n_j} X_{j,i}$ . When both samples have the same covariance matrix a possible estimator for  $\Gamma_A = \Gamma_{\text{POOL}}$  is the pooled covariance operator given by

$$\widehat{\Gamma}_{\text{POOL}} = \frac{n_D}{n} \widehat{\Gamma}_D + \frac{n_H}{n} \widehat{\Gamma}_H,$$

with  $n = n_D + n_H$  and

$$\widehat{\Gamma}_j = \frac{1}{n_j} \sum_{i=1}^{n_j} (X_{j,i} - \bar{X}_j) \otimes (X_{j,i} - \bar{X}_j),$$

while if the practitioner suspects that  $\Gamma_D \neq \Gamma_H$ , it is better to choose

$$\widehat{\Gamma} = \frac{1}{2} \left( \widehat{\Gamma}_D + \widehat{\Gamma}_H \right).$$

We seek for the values  $\widehat{\beta}$  maximizing  $\widehat{L}_\lambda(\beta)$  over the set  $\{\beta \in \mathcal{H}_k : \|\beta\| = 1\}$  with  $\mathcal{H}_k$  a finite-dimensional linear space of dimension  $k$ , such as the one spanned by the first elements of the Fourier basis. An adaptive basis, as the one spanned by the first eigenfunctions of the pooled sample operator may also be chosen. Note that when  $\mathcal{H}_k = \mathcal{H}$ , that is, if no dimension reduction is performed, the procedure corresponds to the optimal scoring approach to discriminant analysis described in [Ramsay and Silverman \(2005\)](#).

As mentioned above, once the direction  $\widehat{\beta}$  is obtained, the estimated discrimination index  $\widehat{\Upsilon}_{\widehat{\beta}}(X) = \langle \widehat{\beta}, X \rangle$  may be constructed, leading to the real-valued samples  $Y_{j,i} = \widehat{\Upsilon}_{\widehat{\beta}}(X_{j,i}) = \langle \widehat{\beta}, X_{j,i} \rangle$ ,  $1 \leq i \leq n_j$ ,  $j = D, H$  from which the ROC curve estimator may be constructed as

$$\widehat{\text{ROC}}(p) = \widehat{\text{ROC}}_{\widehat{\Upsilon}_{\widehat{\beta}}}(p) = 1 - \widehat{F}_D \left( \widehat{F}_H^{-1}(1 - p) \right), \quad p \in (0, 1), \quad (9)$$

where  $\widehat{F}_D = \widehat{F}_{\widehat{\Upsilon}_{\widehat{\beta}}, D}$  and  $\widehat{F}_H^{-1} = \widehat{F}_{\widehat{\Upsilon}_{\widehat{\beta}}, H}^{-1}$  stand for the empirical distribution function and quantile function of the samples  $Y_{j,i}$ ,  $1 \leq i \leq n_j$ ,  $j = D, H$ , respectively.

## 3.2 Definition of a quadratic discrimination index

In the situations where the covariance operators differ between populations, some improvements to the linear index defined above may be obtained in terms of the AUC by considering alternative indexes. As it is well known, for multivariate normally distributed biomarkers the quadratic discriminating rule offers a procedure with better classification rates than the linear one when the covariance matrices of both populations are different from each other, in particular for unbalanced samples.

Measuring differences between covariance operators or even between covariance matrices is difficult, we refer to [Flury \(1988\)](#) who mentioned that “*In contrast to the univariate situation, inequality is not just inequality—there are indeed many ways in which covariance matrices can*

*differ*”. For that reason, some parsimonious models have been considered, including models with proportional covariance operators or models assuming that both covariance operators share the same eigenfunctions. In this section, we focus on these settings and we will use the basis of principal directions to reduce the dimension, even when any basis can be chosen to project the data and construct the quadratic index when we suspect that differences between covariance operators arise.

A natural extension of functional principal components to several populations, which corresponds to the generalization of the common principal components model introduced by [Flury \(1984\)](#) to the functional setting, is to assume that the covariance operators  $\Gamma_j$  have common eigenfunctions  $\phi_\ell$  but possible different eigenvalues  $\lambda_{j,\ell}$ , i.e.,

$$\Gamma_j = \sum_{\ell=1}^{\infty} \lambda_{j,\ell} \phi_\ell \otimes \phi_\ell, \quad (10)$$

where, to identify the directions, we assume that the eigenvalues of the first population are ordered in decreasing order, that is,  $\lambda_{1,1} \geq \lambda_{1,2} \geq \dots \geq \lambda_{1,\ell} \geq \lambda_{1,\ell+1} \dots$ . This model is usually denoted the functional common principal component model (FCPC) and provides a framework for analysing different population data that share their main modes of variation  $\phi_1, \phi_2, \dots$  using a parsimonious approach. When the eigenvalues preserve the order across populations, i.e., if

$$\lambda_{j,1} \geq \lambda_{j,2} \geq \dots \geq \lambda_{j,\ell} \geq \lambda_{j,\ell+1} \dots, \text{ for } j = D, H, \quad (11)$$

as assumed, for instance, in [Benko and Härdle \(2005\)](#) and [Boente et al. \(2010\)](#), the common directions will represent, as in the one–population setting, the main modes of variation for each population. Furthermore, in such a situation, the operators  $\Gamma_{\text{POOL}}$  and  $\Gamma_A$  will also have the same principal directions and in the same order.

However, if the largest  $k$  eigenvalues do not preserve the order among populations, that is, if we only have

$$\lambda_{j,\ell} \geq \lambda_{j,k+1} \geq \lambda_{j,k+2} \geq \dots \geq 0 \quad \text{for } j = D, H \text{ and } 1 \leq \ell \leq k,$$

$\phi_1, \dots, \phi_k$  represent the modes of variation that are common to each group, even when the ordering across groups changes. As mentioned in [Coffey et al. \(2011\)](#), the eigenvalues  $\lambda_{j,\ell}$ ,  $1 \leq \ell \leq k$ , determine the order of the common directions in each group and may allow to

study the differences in the distribution of the variation across groups. The functional common principal component model may be used to reduce the dimensionality of the data, retaining the maximum variability present in each of the populations.

Assume that the covariance operators of both populations satisfy a FCPC model and that (11) holds, then the first  $k$  principal directions provide a natural linear space where the data projection may be performed. More precisely, define the  $k$ -dimensional vectors  $\mathbf{x}_j = (\langle \phi_1, X_j \rangle, \dots, \langle \phi_k, X_j \rangle)^T$ ,  $j = D, H$ , where  $\phi_\ell$ ,  $\ell = 1, \dots, k$ , stand for the first  $k$  common principal directions. Note that when  $X_j$ ,  $j = D, H$ , are Gaussian processes with mean  $\mu_j$  and covariance operators  $\Gamma_j$  satisfying (10), then  $\mathbf{x}_{j,i} \sim N(\boldsymbol{\mu}_j, \boldsymbol{\Sigma}_j)$  with  $\boldsymbol{\mu}_j = (\mu_{j,1}, \dots, \mu_{j,k})^T$ ,  $\mu_{j,\ell} = \langle \phi_\ell, \mu_j \rangle$  and  $\boldsymbol{\Sigma}_j = \text{DIAG}(\lambda_{j,1}, \dots, \lambda_{j,k})$ , meaning that  $\mathbf{x}_{j,1}$ ,  $j = D, H$ , fulfil the common principal components model (CPC) considered in Flury (1984). From these projections, if  $\lambda_{j,k} > 0$ , for  $j = D, H$ , a quadratic discriminant index may be defined as

$$\Upsilon_{\text{QUAD}}(X) = -\mathbf{x}^T \boldsymbol{\Lambda} \mathbf{x} + 2\boldsymbol{\alpha}^T \mathbf{x},$$

where  $\mathbf{x} = (\langle \phi_1, X \rangle, \dots, \langle \phi_k, X \rangle)^T$ ,  $\boldsymbol{\Lambda} = \boldsymbol{\Sigma}_D^{-1} - \boldsymbol{\Sigma}_H^{-1}$  and  $\boldsymbol{\alpha} = \boldsymbol{\Sigma}_D^{-1} \boldsymbol{\mu}_D - \boldsymbol{\Sigma}_H^{-1} \boldsymbol{\mu}_H$ . Note that under the FCPC model

$$\begin{aligned} \boldsymbol{\Lambda} &= \text{DIAG} \left( \frac{\lambda_{H,1} - \lambda_{D,1}}{\lambda_{D,1} \lambda_{H,1}}, \dots, \frac{\lambda_{H,k} - \lambda_{D,k}}{\lambda_{D,k} \lambda_{H,k}} \right) = \text{DIAG}(\Lambda_1, \dots, \Lambda_k) \\ \boldsymbol{\alpha} &= \begin{pmatrix} \frac{\mu_{D,1} \lambda_{H,1} - \mu_{H,1} \lambda_{D,1}}{\lambda_{D,1} \lambda_{H,1}} \\ \vdots \\ \frac{\mu_{D,k} \lambda_{H,k} - \mu_{H,k} \lambda_{D,k}}{\lambda_{D,k} \lambda_{H,k}} \end{pmatrix} = \begin{pmatrix} \frac{\mu_{D,1}}{\lambda_{D,1}} - \frac{\mu_{H,1}}{\lambda_{H,1}} \\ \vdots \\ \frac{\mu_{D,k}}{\lambda_{D,k}} - \frac{\mu_{H,k}}{\lambda_{H,k}} \end{pmatrix}. \end{aligned}$$

Besides,  $\Upsilon_{\text{QUAD}}(X) = \Upsilon_{k,\text{QUAD}}(X)$  since it depends on the number of selected common directions. However, we have decided to omit its dependence on  $k$  to simplify the notation.

Under mild assumptions, Proposition 3.3 below provides an expression of the quadratic discriminating rule which suggests an asymptotic expression for it, as the number of principal directions increases.

**Proposition 3.3.** *Assume that  $\Gamma_j$  satisfy (10) and (11), with  $\lambda_{j,\ell} > 0$ , for  $j = D, H$  and  $\ell \geq 1$ , and that  $\mu_j \in \mathcal{R}(\Gamma_j)$ . Denote  $\boldsymbol{\alpha} = \Gamma_D^{-1} \boldsymbol{\mu}_D - \Gamma_H^{-1} \boldsymbol{\mu}_H$  and let  $A : \mathcal{H} \rightarrow \mathbb{R}^k$  stand for the projection operator  $Ay = (\langle \phi_1, y \rangle, \dots, \langle \phi_k, y \rangle)^T$ , for any  $y \in \mathcal{H}$ . Then,*



a)  $\boldsymbol{\alpha}^T \mathbf{x} = \langle A^* A \boldsymbol{\alpha}, X \rangle = \sum_{\ell=1}^k \langle \boldsymbol{\alpha}, \phi_\ell \rangle \langle \phi_\ell, X \rangle$  where  $A^* : \mathbb{R}^k \rightarrow \mathcal{H}$  stands for the adjoint operator of  $A$  given by  $A^* \mathbf{u} = \sum_{\ell=1}^k u_\ell \phi_\ell$ .

b)  $\mathbf{x}^T \boldsymbol{\Lambda} \mathbf{x} = \|A \Gamma_D^{-1/2} X\|^2 - \|A \Gamma_H^{-1/2} X\|^2$ , if  $X \in \mathcal{R}(\Gamma_D^{1/2}) \cap \mathcal{R}(\Gamma_H^{1/2})$ . Hence,

$$\Upsilon_{\text{QUAD}}(X) = - \left( \|A \Gamma_D^{-1/2} X\|^2 - \|A \Gamma_H^{-1/2} X\|^2 \right) + 2 \langle A^* A \boldsymbol{\alpha}, X \rangle.$$

Then, for any  $X \in \mathcal{R}(\Gamma_D^{1/2}) \cap \mathcal{R}(\Gamma_H^{1/2})$ , if the number  $k$  of principal directions increases to infinity the index  $\Upsilon_{\text{QUAD}}(X)$  converges to  $\Upsilon(X) = - \left( \|\Gamma_D^{-1/2} X\|^2 - \|\Gamma_H^{-1/2} X\|^2 \right) + 2 \langle \boldsymbol{\alpha}, X \rangle$ .

Two facts should be highlighted regarding Proposition 3.3. On the one hand, note that from the Karhunen–Loève expansion of the Gaussian processes  $X_j$ , we get that  $\mathbb{P}(X_j - \mu_j \in \mathcal{R}(\Gamma_j^{1/2})) = 0$ . Effectively, the mentioned expansion leads to  $X_j - \mu_j = \sum_{\ell \geq 1} \xi_{j,\ell} \phi_\ell$  where  $\xi_{j,\ell}$  are independent and  $\xi_{j,\ell} \sim N(0, \lambda_{j,\ell})$  which implies that  $\langle X_j, \phi_\ell \rangle^2 / \lambda_{j,\ell} = \xi_{j,\ell}^2 / \lambda_{j,\ell} \sim \chi_1^2$ , meaning that  $X_j - \mu_j \notin \mathcal{R}(\Gamma_j^{1/2})$  with probability 1. Thus, the linear space where  $\Upsilon$  is defined is too small to define a proper discriminating rule. In this sense,  $\Upsilon_{\text{QUAD}} = \Upsilon_{k,\text{QUAD}}$  circumvents the *curse of dimensionality* imposed by the infinite–dimensional structure of the model and provides a finite–dimensional approximation of  $\Upsilon$  whose range is the whole space  $\mathcal{H}$  ensuring the definition of a proper rule. On the other hand, assumption  $\lambda_{j,\ell} > 0$ , for  $j = D, H$  and  $\ell \geq 1$ , is needed to guarantee that  $\Gamma_j$  has an inverse over  $\mathcal{R}(\Gamma_j)$ . Moreover, if  $\lambda_{j,\ell} = 0$ , for  $\ell \geq k_0$ , then the quadratic rule  $\Upsilon_{k,\text{QUAD}}$  may only be defined when  $k < k_0$ , since otherwise the matrix  $\boldsymbol{\Sigma}_j$  will be singular.

Clearly, the principal directions are unknown and must be estimated from the sample. These estimators denoted  $\widehat{\phi}_\ell$ ,  $\ell = 1, \dots, k$ , may be obtained, for instance, as the eigenfunctions related to the largest  $k$  eigenvalues of the sample pooled covariance operator, see for instance, [Boente et al. \(2010\)](#). We then may define the  $k$ –dimensional vectors  $\widehat{\mathbf{x}}_{j,i} = (\langle \widehat{\phi}_1, X_{j,i} \rangle, \dots, \langle \widehat{\phi}_k, X_{j,i} \rangle)^T$ ,  $1 \leq i \leq n_j$ ,  $j = D, H$ , which provide predictors of the finite–dimensional vectors  $\mathbf{x}_{j,i} = (\langle \phi_1, X_{j,i} \rangle, \dots, \langle \phi_k, X_{j,i} \rangle)^T$ .

In this case, the quadratic discrimination rule provides a better approach to classify a new observation to each group. For that reason, we propose to consider as estimated quadratic index

$$\widehat{\Upsilon}_{\text{QUAD}}(X) = -\mathbf{x}^T \widehat{\boldsymbol{\Lambda}} \mathbf{x} + 2\widehat{\boldsymbol{\alpha}}^T \mathbf{x}, \quad (12)$$

where  $\mathbf{x} = (\langle \hat{\phi}_1, X \rangle, \dots, \langle \hat{\phi}_k, X \rangle)^T$ ,  $\hat{\mathbf{\Lambda}} = \hat{\Sigma}_D^{-1} - \hat{\Sigma}_H^{-1}$ ,  $\hat{\boldsymbol{\alpha}} = \hat{\Sigma}_D^{-1} \hat{\boldsymbol{\mu}}_D - \hat{\Sigma}_H^{-1} \hat{\boldsymbol{\mu}}_H$  where  $\hat{\boldsymbol{\mu}}_j$  and  $\hat{\Sigma}_j$  stand for the sample mean and covariance matrix of  $\{\mathbf{x}_{j,i}\}_{i=1}^{n_j}$ ,  $j = D, H$ , respectively.

Again, the estimated ROC curve may be defined as

$$\widehat{\text{ROC}}(p) = \widehat{\text{ROC}}_{\hat{\Upsilon}_{\text{QUAD}}}(p) = 1 - \hat{F}_D \left( \hat{F}_H^{-1}(1-p) \right), \quad p \in (0, 1), \quad (13)$$

where  $\hat{F}_D = \hat{F}_{\hat{\Upsilon}_{\text{QUAD}}, D}$  and  $\hat{F}_H^{-1} = \hat{F}_{\hat{\Upsilon}_{\text{QUAD}}, H}^{-1}$  denote the empirical distribution function and quantile function of the samples  $Y_{j,i} = \hat{\Upsilon}_{\text{QUAD}}(X_{j,i})$ ,  $1 \leq i \leq n_j$ ,  $j = D, H$ , respectively.

As mentioned in [Flury and Schmid \(1992\)](#), for the multivariate setting, the quadratic rule may be adapted to the setting of CPC or proportional models estimating the parameters under these constraints. This procedure may lead to more stable estimations than those obtained using the sample covariance estimators  $\hat{\Sigma}_j$ , specially for small samples, leading to better rates of misclassification and probably to higher AUC values, when the most parsimonious among all the correct models is used for discrimination. We leave the interesting topic of comparing the performance of the ROC curve estimators obtained using constrained estimators for future research.

## 4 Some consistency results

In this section, we establish consistency results for some discriminating indexes under mild assumptions. In particular, we consider the situation where the index  $\Upsilon(X)$  is linear and defined by means of a coefficient  $\beta_0$  that may be known as in the case of  $\Upsilon(X) = \int_{\mathcal{I}} X(t) dt$  where  $\beta_0 \equiv 1$  or unknown as it arises when considering, for instance,  $\Upsilon(X) = \langle \mu_D - \mu_H, X \rangle$  where  $\beta_0 = \mu_D - \mu_H$  or  $\Upsilon(X) = \langle \beta_0, X \rangle$ , where  $\beta_0$  maximizes  $L_{\text{POOL}}(\beta)$ . We also consider the situation of the quadratic discrimination rule defined in [Section 3.2](#), when the number of principal directions is fixed.

Let  $X_j \sim P_j$ ,  $j = D, H$ , be a multivariate or functional biomarker ( $X_j \in \mathcal{H}$ ). Consider  $\Upsilon : \mathcal{H} \rightarrow \mathbb{R}$  a discrimination index used to define the ROC curve  $\text{ROC}_{\Upsilon}$  as in [\(4\)](#), where for simplicity we denote  $F_j = F_{\Upsilon, j}$  the distribution function of  $Y_j = \Upsilon(X_j)$ ,  $j = D, H$ . Recall that the related area under the curve equals  $\text{AUC}_{\Upsilon} = \mathbb{P}(Y_{\Upsilon, D} > Y_{\Upsilon, H})$ .

The estimator of ROC is obtained in many situations by means of an estimated discrim-

ination index  $\widehat{\Upsilon}$ , unless  $\Upsilon$  is completely known in which case in what follows  $\widehat{\Upsilon} = \Upsilon$ . This estimator is based on independent samples  $X_{j,i}$ ,  $1 \leq i \leq n_j$ ,  $j = D, H$ , which allow to define  $\widehat{ROC} = \widehat{ROC}_{\widehat{\Upsilon}}$  and  $\widehat{AUC} = \widehat{AUC}_{\widehat{\Upsilon}}$  as in (6) and (7), respectively. For simplicity, we label  $\widehat{F}_j = \widehat{F}_{\widehat{\Upsilon},j}$  for the empirical distribution function of the samples  $\widehat{Y}_{j,i} = \widehat{\Upsilon}(X_{j,i})$ ,  $1 \leq i \leq n_j$ ,  $j = D, H$ . It is worth noting that the asymptotic results we derive are based on the assumption that sample sizes grow to infinity, that is  $n_j \rightarrow \infty$ ,  $j = D, H$ .

In order to derive consistency results for the ROC curve estimators  $\widehat{ROC}_{\widehat{\Upsilon}}$ , we will need the following assumptions.

**A1**  $F_H = F_{H,\Upsilon} : \mathbb{R} \rightarrow (0, 1)$  has density  $f_{H,\Upsilon}$  such that  $f_{H,\Upsilon}(u) > 0$ , for all  $u \in \mathbb{R}$ .

**A2**  $F_D = F_{D,\Upsilon} : \mathbb{R} \rightarrow (0, 1)$  is continuous.

**A3**  $\|\widehat{F}_j - F_j\|_{\infty} \xrightarrow{a.s.} 0$ ,  $j = D, H$ .

Theorem 4.1 below provides conditions ensuring that the resulting estimators of the ROC curve are consistent.

**Theorem 4.1.** *Let  $\{X_{j,i}\}_{1 \leq i \leq n_j}$ ,  $j = D, H$ , be independent observations and let  $\widehat{\Upsilon}$  an estimator of  $\Upsilon$ . Assume that **A1** to **A3** hold. Then,*

$$(a) \sup_{0 < p < 1} |\widehat{ROC}(p) - ROC(p)| \xrightarrow{a.s.} 0,$$

$$(b) \widehat{AUC} \xrightarrow{a.s.} AUC,$$

$$(c) \widehat{YI} \xrightarrow{a.s.} YI.$$

**Remark 4.1.** *Note that the Glivenko–Cantelli Theorem entails that **A3** holds when  $\Upsilon$  is known. Hence, when the discriminating index is linear  $\Upsilon(X) = \langle \beta_0, X \rangle$  where  $\beta_0$  is known, Theorem 4.1 provides mild conditions ensuring consistency of the estimated ROC curve.*

*More precisely, if the distribution function  $F_{j,\Upsilon}$  of  $Y_j = \Upsilon(X_j)$  are continuous, for  $j = D, H$ , and  $F_{H,\Upsilon}$  has density  $f_{H,\Upsilon}$  such that  $f_{H,\Upsilon}(u) > 0$ , for all  $u \in \mathbb{R}$ , then the conclusion of Theorem 4.1 holds for the estimator given in (5).*

*Theorem 4.1 also provides consistency results for the discriminating indexes defined in Jang and Mantunga (2022),  $\Upsilon(X) = \int_{\mathcal{I}} X(t)dt$ ,  $\Upsilon(X) = \int_{\mathcal{I}} X'(t)dt = X(b) - X(a)$ ,  $\Upsilon(X) = \int_{\mathcal{I}} X''(t)dt = X'(b) - X'(a)$  as well as  $\Upsilon(X) = \max_{t \in \mathcal{I}} X(t)$  and  $\Upsilon(X) = \min_{t \in \mathcal{I}} X(t)$ .*

By means of Theorem 4.1, Theorems 4.2 and 4.3 state consistency results when the discriminating index is linear. More precisely, let  $\beta_0$  be the direction in which we project in order to determine the ROC curve, i.e., we assume that  $\Upsilon(X) = \langle \beta_0, X \rangle$ . Furthermore, denote  $\Upsilon_\beta(X) = \langle X, \beta \rangle$  and  $F_{\beta,j} = F_{\Upsilon_{\beta,j}}$  the distribution of  $\Upsilon_\beta(X_j)$  when  $X_j \sim P_j$ , while for simplicity, as above, we will call  $F_j$  that corresponding to  $F_{\beta_0,j}$ .

From now on,  $\widehat{\beta}$  stand for an estimator of  $\beta_0$  which we will assume to be consistent. We denote  $\widehat{F}_{\beta,j} = \widehat{F}_{\Upsilon_{\beta,j}}$  the empirical distribution related of  $\Upsilon_\beta(X_{j,i}) = \langle X_{j,i}, \beta \rangle$ ,  $1 \leq i \leq n_j$ ,  $j = D, H$ , while, to abbreviate,  $\widehat{F}_j$  stands for  $\widehat{F}_{\beta_0,j}$ . The ROC curve associated to  $\Upsilon(X) = \Upsilon_{\beta_0}(X) = \langle \beta_0, X \rangle$  can be written as  $\text{ROC}(p) = 1 - F_D(F_H^{-1}(1-p))$ , while its estimator equals  $\widehat{\text{ROC}}(p) = 1 - \widehat{F}_D(\widehat{F}_H^{-1}(1-p))$ . Without loss of generality, we may assume that  $\|\beta_0\| = 1$  and  $\|\widehat{\beta}\| = 1$ .

Assumptions **A1** and **A2** state that  $F_{\beta_0,j}$  are continuous for  $j = D, H$  and  $F_{\beta_0,H}$  has a strictly positive density  $f_{\beta_0,H}$ . The key point is to provide conditions ensuring that **A3** holds.

In the finite-dimensional setting, Theorem 4.2 ensures that **A3** is a consequence of the strong consistency of  $\widehat{\beta}$ , while Theorem 4.3 extends the result to the case of an infinite-dimensional biomarker requiring a finite expansion for the possible estimators  $\widehat{\beta}$ . In Theorem 4.2 below, to strengthen the fact that we are dealing with finite-dimensional observations, the biomarkers and the index coefficient are indicated with boldface.

**Theorem 4.2.** *Assume that  $\mathcal{H} = \mathbb{R}^k$  and let  $\{\mathbf{x}_{j,i}\}_{1 \leq i \leq n_j}$ ,  $j = D, H$ , be independent observations in  $\mathbb{R}^k$ . Let  $\widehat{\beta}$  a strongly consistent estimator of  $\beta_0$  and assume that  $F_{\beta_0,j}$  are continuous for  $j = D, H$ . Then,*

- a) **A3** holds.
- b) *If in addition  $F_{\beta_0,H}$  has density  $f_{\beta_0,H}$  such that  $f_{\beta_0,H}(u) > 0$ , for all  $u \in \mathbb{R}$ , then the conclusion of Theorem 4.1 holds.*

Let us consider now the situation of a separable Hilbert space, where the estimator  $\widehat{\beta}$  is obtained using finite-dimensional candidates obtained from a fixed basis. More precisely, assume that

$$\widehat{\beta} = \sum_{s=1}^k \widehat{b}_s \phi_s, \quad (14)$$

where the coefficients  $\widehat{b}_s$ ,  $s = 1, \dots, k$ , are data-dependent and the dimension  $k = k_n$  increases with the sample size  $n = n_D + n_H$ .

**Theorem 4.3.** *Let  $\{X_{j,i}\}_{1 \leq i \leq n_j}$ ,  $j = D, H$ , be independent observations in a separable Hilbert space  $\mathcal{H}$  and let  $\widehat{\beta}$  in (14) be an estimator of  $\beta_0$  such that  $\|\widehat{\beta} - \beta_0\| \xrightarrow{a.s.} 0$  and  $k_n/n \rightarrow 0$  and assume that  $F_{\beta_0,j}$  are continuous for  $j = D, H$ . Then,*

a) **A3** holds.

b) *If in addition  $F_{\beta_0,H}$  has density  $f_{\beta_0,H}$  such that  $f_{\beta_0,H}(u) > 0$ , for all  $u \in \mathbb{R}$ , then the conclusion of Theorem 4.1 holds.*

To derive consistency results for the ROC curve associated to  $\widehat{\Upsilon}_{\text{QUAD}}$  given in (12), we will consider general quadratic indexes defined as  $\Upsilon_{\mathbf{\Lambda}, \mathbf{\alpha}}(X) = -\mathbf{x}^T \mathbf{\Lambda} \mathbf{x} + \mathbf{\alpha}^T \mathbf{x}$  where  $\mathbf{x} = A(X) = (\langle X, \phi_1 \rangle, \dots, \langle X, \phi_k \rangle)^T$ ,  $\mathbf{\alpha} \in \mathbb{R}^k$  and  $\mathbf{\Lambda} \in \mathbb{R}^{k \times k}$  and  $\{\phi_\ell\}_{\ell \geq 1}$  is an orthonormal basis of  $\mathcal{H}$ . To avoid heavy the notation, we have omitted the index  $k$  related to the number of principal directions chosen which will be assumed to be fixed. As above, we assume that the index  $\Upsilon$  used to construct the ROC curve equals  $\Upsilon = \Upsilon_{\mathbf{\Lambda}_0, \mathbf{\alpha}_0}$  for some squared matrix  $\mathbf{\Lambda}_0$  and vector  $\mathbf{\alpha}_0$ . We also assume that estimators  $(\widehat{\mathbf{\Lambda}}, \widehat{\mathbf{\alpha}})$  of  $(\mathbf{\Lambda}_0, \mathbf{\alpha}_0)$  are available and that the estimated ROC curve is defined through the samples  $\widehat{Y}_{j,i} = \widehat{\Upsilon}(X_{j,i})$ ,  $1 \leq i \leq n_j$ ,  $j = D, H$ , where  $\widehat{\Upsilon} = \Upsilon_{\widehat{\mathbf{\Lambda}}, \widehat{\mathbf{\alpha}}}$  as in (5). As for the linear index, assumption **A3** will follow from the consistency of  $(\widehat{\mathbf{\Lambda}}, \widehat{\mathbf{\alpha}})$ .

Again, **A1** and **A2** state assumptions on the behaviour of the distribution functions  $F_j = F_{j, \Upsilon_{\mathbf{\Lambda}_0, \mathbf{\alpha}_0}}$  of  $Y_j = \Upsilon(X_j) = \Upsilon_{\mathbf{\Lambda}_0, \mathbf{\alpha}_0}(X_j)$  which are the usual requirements to establish consistency for univariate biomarkers. Hence, we have the following result.

**Theorem 4.4.** *Let  $\{X_{j,i}\}_{1 \leq i \leq n_j}$ ,  $j = D, H$ , be independent observations in a separable Hilbert space  $\mathcal{H}$  and let  $(\widehat{\mathbf{\Lambda}}, \widehat{\mathbf{\alpha}})$  strongly consistent estimators of  $(\mathbf{\Lambda}_0, \mathbf{\alpha}_0)$  and assume that  $F_j$  are continuous. Then,*

a) **A3** holds.

b) *If in addition  $F_H = F_{H, \Upsilon_{\mathbf{\Lambda}_0, \mathbf{\alpha}_0}}$  has density  $f_H$  such that  $f_H(u) > 0$ , for all  $u \in \mathbb{R}$ , the conclusion of Theorem 4.1 holds.*

## 5 Monte Carlo Study

In this section, we report the results of a numerical study performed with the aim of comparing different rules used to define an estimator of the ROC curve. In particular, we consider the estimators defined through (9) and (13). The estimator defined in (9) may also be used when  $\beta(t) = 1$  for all  $t$ , which leads to the ROC curve based on the integral-type index labelled  $\Upsilon_I(X) = \int_{\mathcal{I}} X(t)dt$  used in Jang and Mantunga (2022). Beyond these discriminating indexes, the maximum and the minimum of each trajectory are also used as discriminating rule, that is, the ROC curve is based on  $\Upsilon_{\text{MAX}}(X_{j,i})$  or  $\Upsilon_{\text{MIN}}(X_{j,i})$ ,  $1 \leq i \leq n_j$ ,  $j = D, H$ , where  $\Upsilon_{\text{MAX}}(X) = \max_{t \in \mathcal{I}} X(t)$  and  $\Upsilon_{\text{MIN}}(X) = \min_{t \in \mathcal{I}} X(t)$ . Furthermore, we label as  $\Upsilon_M(X) = \langle \mu_D - \mu_H, X \rangle$  the linear discriminating rule based on the mean difference that will be estimated by  $\langle \bar{X}_D - \bar{X}_H, X \rangle$ . We also consider the linear discriminating rule labelled  $\Upsilon_{\text{LIN}}(X) = \langle \beta_{\text{LIN}}, X \rangle$ , where  $\beta_{\text{LIN}}$  maximizes  $L(\beta)$ , defined in (8), over  $\|\beta\| = 1$ . The estimator of  $\beta_{\text{LIN}}$  is obtained by maximizing

$$\hat{L}(\beta) = \frac{\langle \beta, \hat{\mu}_D - \hat{\mu}_H \rangle}{\left[ \langle \beta, \hat{\Gamma}_A \beta \rangle \right]^{\frac{1}{2}}}$$

over  $\{\beta \in \mathcal{H}_k : \|\beta\| = 1\}$ , where  $\mathcal{H}_k$  is the linear space spanned by the first  $k$  eigenfunctions of the pooled covariance operator

$$\hat{\Gamma}_{\text{POOL}} = \frac{n_D}{n} \hat{\Gamma}_D + \frac{n_H}{n} \hat{\Gamma}_H,$$

with  $\hat{\Gamma}_j$  the sample covariance operators of the  $j$ -th sample,  $j = D, H$  and  $n = n_D + n_H$ . The operator  $\hat{\Gamma}_A$  equals  $(\hat{\Gamma}_D + \hat{\Gamma}_H)/2$ . In all cases, the dimension  $k$  is chosen as the smallest dimension ensuring that at least a 95% of the total variability is explained, measured through the eigenvalues of  $\hat{\Gamma}_{\text{POOL}}$ .

We include also in the comparison the quadratic discriminating rule defined in (12) that will be labelled  $\Upsilon_{\text{QUAD}}$ , to avoid burden notation.

The results for the AUC and ROC curve estimators obtained using each discriminating index are indicated in all Tables and Figures through the considered index.

We consider several frameworks including equal or different covariance operators as well as equal or different mean functions.

Sections 5.1 and 5.2 report the obtained results for different Gaussian processes, when

differences between mean curves are present and for equal mean functions. For all scenarios, we performed 1000 replications where the trajectories were recorded over a grid of 100 points equally spaced on  $[0, 1]$ . The estimated ROC curves were computed over a grid of 101 points equally spaced on  $[0, 1]$ . In Section 5.1, we consider equal sample sizes for both populations,  $n_D = n_H = 300$ , while Section 5.2 is concerned with an unbalanced design,  $n_D = 30$  and  $n_H = 250$  and a setting with proportional covariance operators.

## 5.1 Numerical results for balanced designs

In this section we analyse the performance of the discriminating indexes mentioned above for different Gaussian processes. In all settings  $\mu_H(t) = 0$ , so that the possible differences between mean functions is given through  $\mu_D$ , which varies across scenarios.

We describe below the different scenarios considered.

**PROP** This scenario corresponds to the case of proportional covariance operators  $\Gamma_D = \rho\Gamma_H$ . When  $\rho = 1$  it corresponds to the situation of equal covariance operators. In this last setting, the linear discriminating rule  $\Upsilon_{\text{LIN}}$  usually improves the quadratic one in the multivariate setting for different mean functions.

We consider the case of equal and different mean functions, that will be labelled **P0** and **P1**.

**P0** Under this setting,  $\mu_D(t) = \mu_H(t) = 0$  and  $\Gamma_D = \rho\Gamma_H$  with  $\rho = 2$ .

**P1** In this case,  $\mu_D(t) = 2 \sin(\pi t)$  and  $\Gamma_D = \rho\Gamma_H$  with  $\rho = 1$  and 2.

In these two scenarios both populations have the same underlying Gaussian distribution up to changes in the mean and/or covariance operators.

Two possible Gaussian processes were selected: the Brownian motion and a random Gaussian process with exponential kernel, labelled Exponential Variogram in all Tables and Figures. For the former, covariance kernel for the healthy population equals  $\gamma_H(s, t) = \min(s, t)$ , while for the latter it corresponds to  $\gamma_H(s, t) = \exp(-|s - t|/\theta)$  with  $\theta = 0.2$ .

**CPC** This scenario corresponds to the situation where the covariance operators satisfy a FCPC model. The sample  $X_{H,i}$ ,  $1 \leq i \leq n_H$ , was generated as a Brownian motion with kernel

$\gamma_H(s, t) = \min(s, t)$ . Recall that the eigenfunctions of the Brownian covariance operator are  $\phi_\ell(t) = \sqrt{2} \sin((2\ell - 1)\pi t/2)$  with related principal values  $\lambda_{H,\ell} = 10 [2/\{(2\ell - 1)\pi\}]^2$ .

The diseased population is a finite-range one, generated as  $X_{D,i} = \mu_D + Z_{1,i}\phi_1 + Z_{2,i}\phi_2 + Z_{3,i}\phi_3$ , where  $Z_{\ell,i} \sim N(0, \lambda_{D,\ell})$ , with two possible choices for the variances of the scores.

**C1** In the first one,  $\lambda_{D,1} = 2$ ,  $\lambda_{D,2} = 0.3$  and  $\lambda_{D,3} = 0.05$ . In this situation the order between eigenvalues is preserved across populations.

**C2** For the second choice,  $\lambda_{D,1} = 0.3$ ,  $\lambda_{D,2} = 2$  and  $\lambda_{D,3} = 0.05$ . Note that, in this setting, the order between eigenvalues is not preserved, meaning that the vectors  $\mathbf{x}_j = (\langle \phi_1, X_{j,1} \rangle, \langle \phi_2, X_{j,1} \rangle, \langle \phi_3, X_{j,1} \rangle)^T$  will be normally distributed with diagonal covariance matrices  $\text{DIAG}(\lambda_{j,1}, \lambda_{j,2}, \lambda_{j,3})$ , but the order between the first two principal axes is reversed between populations.

For each of the above described schemes, we allow for two different mean settings. On the one hand, we labelled with a 0 after its identifier, that is, according to the choice of  $\lambda_{D,\ell}$ , for  $\ell = 1, 2, 3$ , as **C10** or **C20** the situation where  $\mu_D(t) = 0$ , for all  $t \in (0, 1)$ . On the other hand, the cases **C11** or **C21** correspond to the situation where the diseased population has mean  $\mu_D(t) = 3 \sin(\pi t)$ .

**DIFF** We also consider a situation where the processes have different covariance operators and do not share their eigenfunctions. Hence, this framework is not included in the proportional or FCPC models described above. Scheme **DIFF** includes two different settings, but in both of them, the sample  $X_{D,i}$ ,  $1 \leq i \leq n_D$ , was generated as a Brownian motion with kernel  $\gamma_H(s, t) = \min(s, t)$ , whereas the sample  $X_{H,i}$ ,  $1 \leq i \leq n_H$ , was generated as described below.

**D1** Under **D1**, the healthy population corresponds to an Ornstein Uhlenbeck process with mean  $\mu_H \equiv 0$  and covariance kernel

$$\gamma_H(s, t) = \frac{1}{2\theta} \exp(-\theta(s + t)) \{ \exp(2\theta(s + t)) - 1 \},$$

with  $\theta = 1/3$ .

**D2** In this framework,  $X_{H,i}$  is distributed as a centered Exponential Variogram, that is,  $\gamma_H(s, t) = \exp(-|s - t|/\theta)$  with  $\theta = 0.2$  and  $\mu_H(t) = 0$ , for all  $t$ .



As above, we include two different mean scenarios: the one labelled a 0 after its identifier, that is, as **D10** or **D20** corresponds to the situation where  $\mu_H(t) = \mu_D(t) = 0$ , for all  $t \in (0, 1)$ . In contrast, the cases **D11** or **D21** correspond to the situation where  $\mu_H(t) = 0$  and the diseased population has mean  $\mu_D(t) = 2 \sin(\pi t)$ .

Figures 2 and 3 depicts 30 trajectories generated for the healthy and diseased populations in blue and red lines, respectively, under the schemes **PROP** and **CPC**, while Figure 4 displays some of the generated trajectories for each scenario in **DIFF**. The true mean functions  $\mu_H$  and  $\mu_D$  are plotted in cyan and orange lines. Figures 2 and 3 reveal that when  $\mu_H = \mu_D = 0$ , the differences between the two underlying distributions are more difficult to detect under the proportional model with  $\rho = 2$  than under the FCPC model. Under the considered FCPC model, the smoothness and the differences in the range of the trajectories allow to distinguish the two populations. We do not consider the scheme,  $\mu_D(t) = \mu_H(t) = 0$  and  $\Gamma_D = \rho \Gamma_H$  with  $\rho = 1$ , since in this case both populations have the same distribution. For that reason in Table 1 below the cells corresponding to **P0** and  $\rho = 1$  are empty. Besides, when both population means are equal, under scenario **D20** the populations may be easily discriminated by looking at their behaviour at  $t = 0$ , in contrast scheme **D10** seems more challenging.

Table 1 and Table 2 report the mean and standard deviations over replications of the AUC estimators under scenarios **PROP** and **CPC**, while Table 3 displays the same summary measures under under scenario **DIFF**. To facilitate the reading we indicate in boldface the largest value attained for the mean of the AUC and in italic, the second largest. The obtained results reveal that in all cases, the best performance is obtained by the quadratic rule,  $\Upsilon_{\text{QUAD}}$ , followed in most situations by the linear one induced by the coefficient maximizing  $\text{AUC}(\beta)$  as defined in Section 3.1, that is, by  $\Upsilon_{\text{LIN}}$ . It is worth mentioning that under the proportional model when the means of both populations are equal or when means are different but the underlying process is an Exponential Variogram, the rule  $\Upsilon_{\text{MAX}}$  based on the maximum value of the trajectory achieves a larger mean value of the AUC estimators than  $\Upsilon_{\text{LIN}}$ , a fact that is clearly revealed in Figure 5 that presents the boxplots of the AUC estimators. When the mean functions are equal, the discriminating indexes based on a linear rule,  $\Upsilon_{\text{I}}$ ,  $\Upsilon_{\text{M}}$  and  $\Upsilon_{\text{LIN}}$ , barely exceed an average estimated AUC of 0.5. The rule based on the maximum has a much better performance under **C20** than under **C10**, while under a proportional model with equal

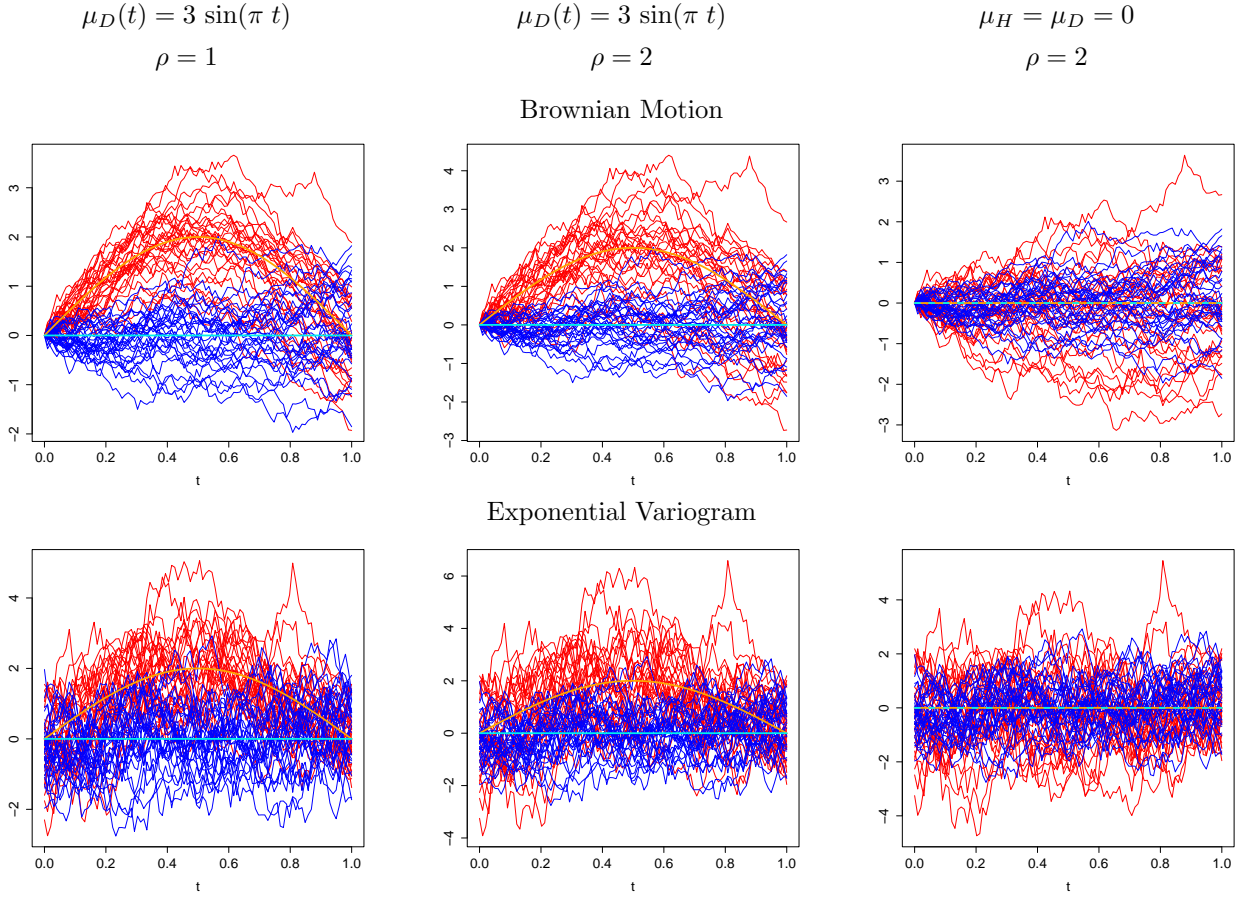


Figure 2: Data sets for proportional models (scheme **PROP**). Blue and red lines correspond to  $X_{H,i}$  and  $X_{D,i}$ , respectively, while the true mean functions  $\mu_H$  and  $\mu_D$  are depicted in cyan and orange lines.

means (**P0**), the differences between populations seem to be more easily detected by  $\Upsilon_{\text{MAX}}$  for the Exponential Variogram process than for the Brownian one. To appreciate the performance differences when the models vary, Figures 6 and 7 display the boxplots of the AUC estimators under the FCPC model and under scheme **DIFF**. It is evident from these plots that scheme **D10** is the more challenging one and only for  $\Upsilon_{\text{QUAD}}$  most estimators are larger than 0.55. There are several simulation scenarios where the obtained AUCs are clearly below 0.5. For example,  $\Upsilon_{\text{MIN}}$  achieves 0.2823 and 0.2647 under **P0** (Exponential Variogram,  $\rho = 2$ ) and **C20**, respectively. This means in fact that, if the roles of the healthy and diseased populations are interchanged, the corresponding rule would achieve AUCs of  $1 - 0.2823$  and  $1 - 0.2647$ , respectively. These values are similar to the ones of  $\Upsilon_{\text{MAX}}$  under the same simulation scenarios. Analogous comments can be done for  $\Upsilon_{\text{MAX}}$  under **D20**, which yields an AUC of 0.1486.

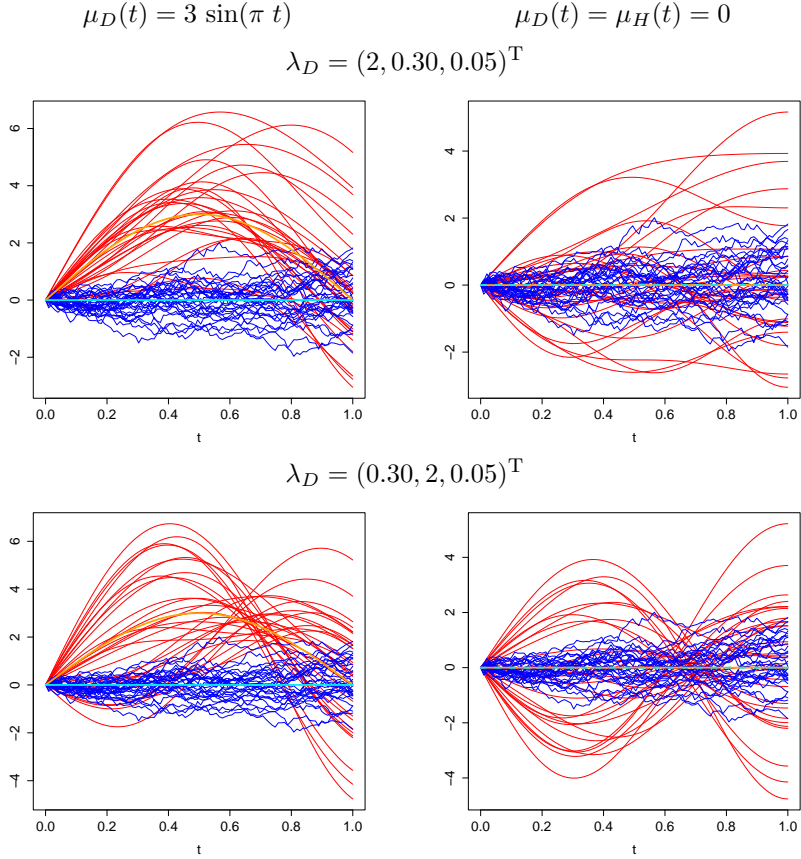


Figure 3: Data sets for under a FCPC model. Blue and red lines correspond to  $X_{H,i}$  and  $X_{D,i}$ , respectively, while the true mean functions  $\mu_H$  and  $\mu_D$  are depicted in cyan and orange lines. The left panel corresponds to the situation of different mean functions and the right one to  $\mu_D(t) = \mu_H(t) = 0$ .

Figures 8 and 9 display the functional boxplots, as defined in Sun and Genton (2011), of the  $n_R = 1000$  realizations of the different estimators of the ROC curve under models **P0** and **P1** with  $\rho = 2$ . We do not show the results for  $\Upsilon_{\text{MIN}}$  since it corresponds to the procedure with the worst performance. In these plots, the magenta central box represents the 50% inner band of curves, the solid black line indicates the central (deepest) function and the dotted red lines indicate outlying curves (in this case: outlying estimates  $\widehat{\text{ROC}}_j$  for some  $1 \leq j \leq n_R$ ). The blue lines correspond to the envelopes, that is, the whiskers in the univariate boxplot and demarcate the limits for a curve to be identified as atypical. The diagonal, in gold color, is shown for comparison purposes. Similarly, Figures 10 and 11 display the functional boxplots under the FCPC model and Figures 12 and 13 the corresponding ones under schemes **D1** and **D2**, respectively.

The behaviour observed in the functional boxplots is consistent with that of the AUC

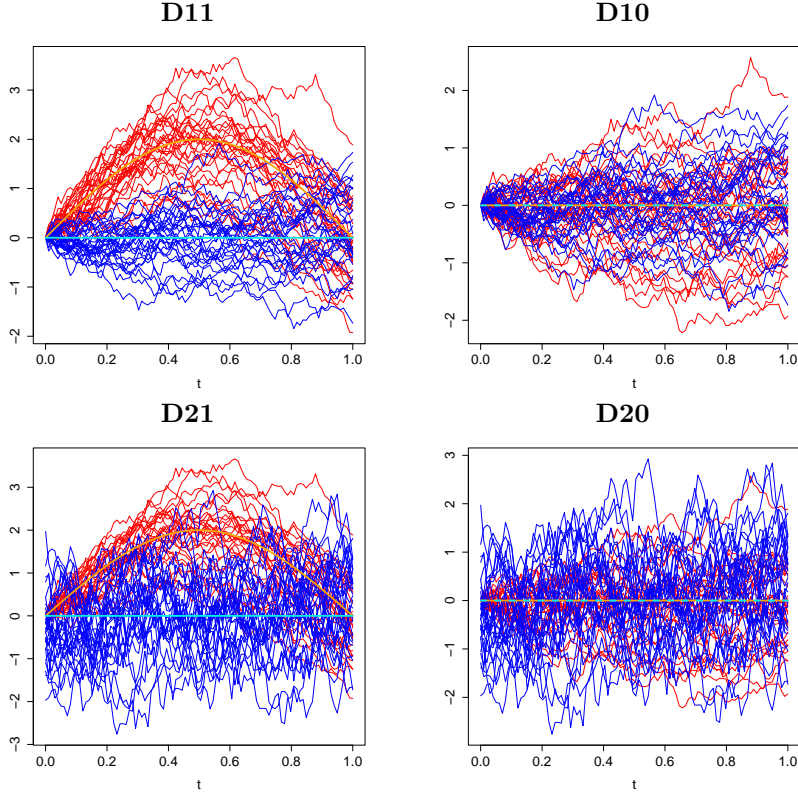


Figure 4: Data sets for under scheme **DIFF**. The left panel corresponds to the case  $\mu_H(t) = 0$  and  $\mu_D(t) = 3 \sin(\pi t)$  and the right one to  $\mu_D(t) = \mu_H(t) = 0$ . Blue and red lines correspond to  $X_{H,i}$  and  $X_{D,i}$ , respectively, while the true mean functions  $\mu_H$  and  $\mu_D$  are depicted in cyan and orange lines.

estimators. When the populations have equal mean, for the linear indexes,  $\Upsilon_I$ ,  $\Upsilon_M$  and  $\Upsilon_{LIN}$ , the central region containing the 50% deepest ROC curve estimators includes or crosses the identity function, except under the proportional model when considering the Exponential Variogram where the ROC curve estimators associated to  $\Upsilon_M$  and  $\Upsilon_{LIN}$  exceed the diagonal for values of  $p$  smaller than 0.4. The worst scenarios for these rules seem to be the FCPC model under **C10**, when  $\lambda_D = (2, 0.30, 0.05)^T$ , and under scheme **D20** for which  $X_D$  follows a Brownian motion and  $X_H$  an Exponential Variogram. The quadratic index results in the best discriminating index for the considered simulation schemes, providing a perfect rule under **D2**.

$\rho$		$\Upsilon_{\text{MAX}}$	$\Upsilon_{\text{MIN}}$	$\Upsilon_{\text{I}}$	$\Upsilon_{\text{M}}$	$\Upsilon_{\text{LIN}}$	$\Upsilon_{\text{QUAD}}$	$\Upsilon_{\text{MAX}}$	$\Upsilon_{\text{MIN}}$	$\Upsilon_{\text{I}}$	$\Upsilon_{\text{M}}$	$\Upsilon_{\text{LIN}}$	$\Upsilon_{\text{QUAD}}$
		<b>P1</b>						<b>P0</b>					
		Brownian Motion											
1	Mean	0.9520	0.6963	0.9389	0.9653	<i>0.9892</i>	<b>0.9987</b>						
	SD	0.0083	0.0219	0.0094	0.0057	0.0004	0.0007						
2	Mean	0.9434	0.6183	0.8965	0.9309	<i>0.9845</i>	<b>0.9945</b>	<i>0.5977</i>	0.4025	0.4998	0.5307	0.5465	<b>0.7648</b>
	SD	0.0091	0.0237	0.0133	0.0090	0.0017	0.0022	0.0239	0.0233	0.0244	0.0136	0.0165	0.0229
		Exponential Variogram											
1	Mean	0.9200	0.7653	0.9426	0.9616	<i>0.9644</i>	<b>0.9809</b>						
	SD	0.0108	0.0191	0.0090	0.0068	0.0051	0.0045						
2	Mean	<i>0.9520</i>	0.5511	0.9011	0.9259	0.9349	<b>0.9905</b>	<i>0.7179</i>	0.2823	0.5000	0.5575	0.6005	<b>0.9627</b>
	SD	0.0082	0.0242	0.0128	0.0107	0.0088	0.0031	0.0212	0.0211	0.0244	0.0134	0.0165	0.0069

Table 1: Mean and standard deviation of the  $\widehat{\text{AUC}}$ , under scenario **PROP**, that is, under a proportional model  $\gamma_D(t, s) = \rho \gamma_H(t, s)$  with equal (**P0**) or different mean functions (**P1**,  $\mu_H(t) = 0$  and  $\mu_D(t) = 2 \sin(\pi, t)$ ). In all cases,  $n_H = n_D = 300$ .

	$\Upsilon_{\text{MAX}}$	$\Upsilon_{\text{MIN}}$	$\Upsilon_{\text{I}}$	$\Upsilon_{\text{M}}$	$\Upsilon_{\text{LIN}}$	$\Upsilon_{\text{QUAD}}$	$\Upsilon_{\text{MAX}}$	$\Upsilon_{\text{MIN}}$	$\Upsilon_{\text{I}}$	$\Upsilon_{\text{M}}$	$\Upsilon_{\text{LIN}}$	$\Upsilon_{\text{QUAD}}$
	$\lambda_D = (2, 0.30, 0.05)^T$											
	<b>C11</b>						<b>C10</b>					
Mean	0.9417	0.6103	0.9099	0.9417	<i>0.9853</i>	<b>0.9905</b>	0.5248	0.4723	0.4985	0.5266	<i>0.5291</i>	<b>0.8531</b>
SD	0.0101	0.0257	0.0132	0.0093	0.0049	0.0038	0.0248	0.0253	0.0247	0.0154	0.0174	0.0160
	$\lambda_D = (0.30, 2, 0.05)^T$											
	<b>C21</b>						<b>C20</b>					
Mean	<i>0.9922</i>	0.5355	0.9856	0.9810	0.9881	<b>0.9966</b>	<i>0.7340</i>	0.2647	0.4991	0.5296	0.5295	<b>0.9090</b>
SD	0.0024	0.0250	0.0036	0.0046	0.0031	0.0013	0.0214	0.0207	0.0239	0.0166	0.0166	0.0126

Table 2: Mean and standard deviation of the  $\widehat{\text{AUC}}$ , under scenario **CPC**, which corresponds to processes with different mean functions  $\mu_H(t) = 0$  and  $\mu_D(t) = 3 \sin(\pi, t)$  (**C11** and **C21**) or equal means (**C10** and **C20**). In all cases,  $n_H = n_D = 300$ .

	$\Upsilon_{\text{MAX}}$	$\Upsilon_{\text{MIN}}$	$\Upsilon_{\text{I}}$	$\Upsilon_{\text{M}}$	$\Upsilon_{\text{LIN}}$	$\Upsilon_{\text{QUAD}}$	$\Upsilon_{\text{MAX}}$	$\Upsilon_{\text{MIN}}$	$\Upsilon_{\text{I}}$	$\Upsilon_{\text{M}}$	$\Upsilon_{\text{LIN}}$	$\Upsilon_{\text{QUAD}}$
	<b>D11</b>						<b>D10</b>					
Mean	0.9607	0.6956	0.9454	<i>0.9695</i>	<b>0.9988</b>	<b>0.9988</b>	0.5048	0.4953	0.4996	0.5314	<i>0.5486</i>	<b>0.5989</b>
SD	0.0072	0.0221	0.0088	0.0053	0.0007	0.0007	0.0244	0.0238	0.0242	0.0130	0.0163	0.0187
	<b>D21</b>						<b>D20</b>					
Mean	0.7370	0.9123	0.9407	0.9634	<i>0.9844</i>	<b>1.0000</b>	0.1486	0.8512	0.4996	0.5491	<i>0.5864</i>	<b>1.0000</b>
SD	0.0207	0.0118	0.0092	0.0064	0.0042	0.0000	0.0154	0.0159	0.0242	0.0140	0.0180	0.0002

Table 3: Mean and standard deviation of the  $\widehat{\text{AUC}}$ , under scenario **DIFF**, when different covariance operators are considered. Under **D11** and **D21**,  $\mu_H(t) = 0$  and  $\mu_D(t) = 2 \sin(\pi, t)$ , while for the schemes **D10** and **D20**  $\mu_D = \mu_H \equiv 0$ . In all cases,  $n_H = n_D = 300$ .

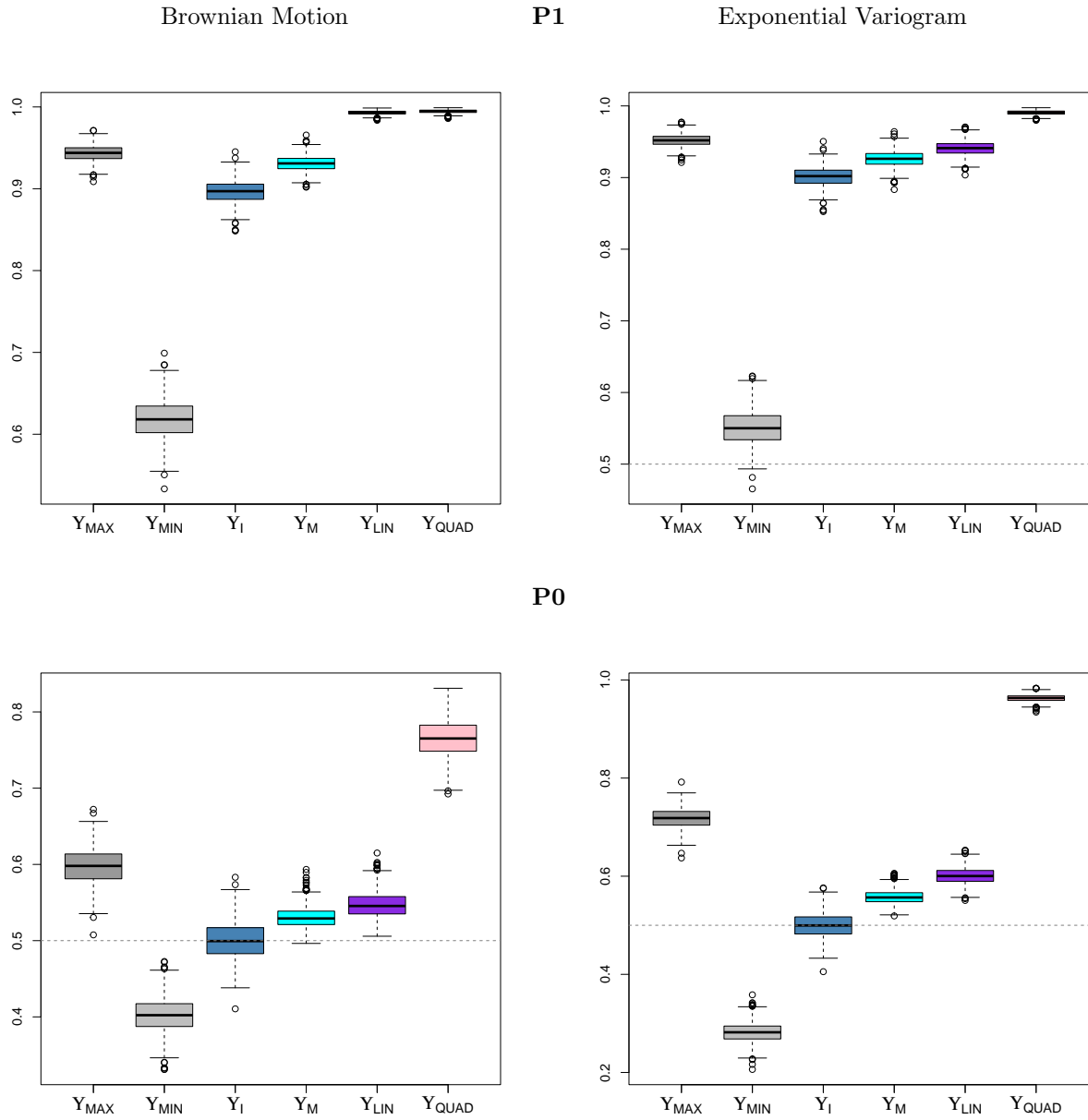


Figure 5: Boxplot of the estimators of the AUC under scenario **PROP** with  $\rho = 2$ . The horizontal dashed line, when appearing, indicates 0.5.

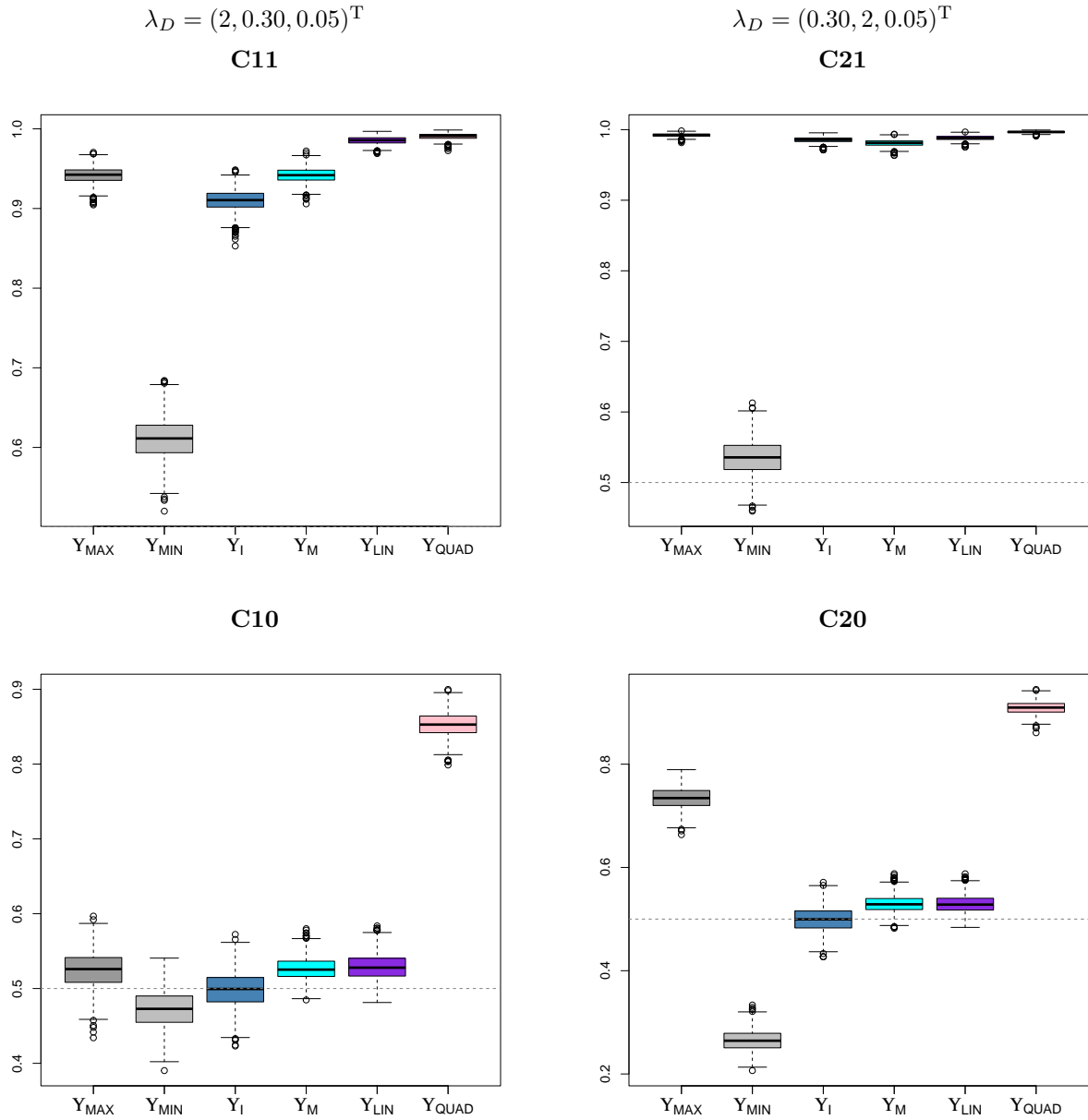


Figure 6: Boxplot of the estimators of the AUC under scenario **CPC**. The horizontal dashed line, when appearing, indicates 0.5.



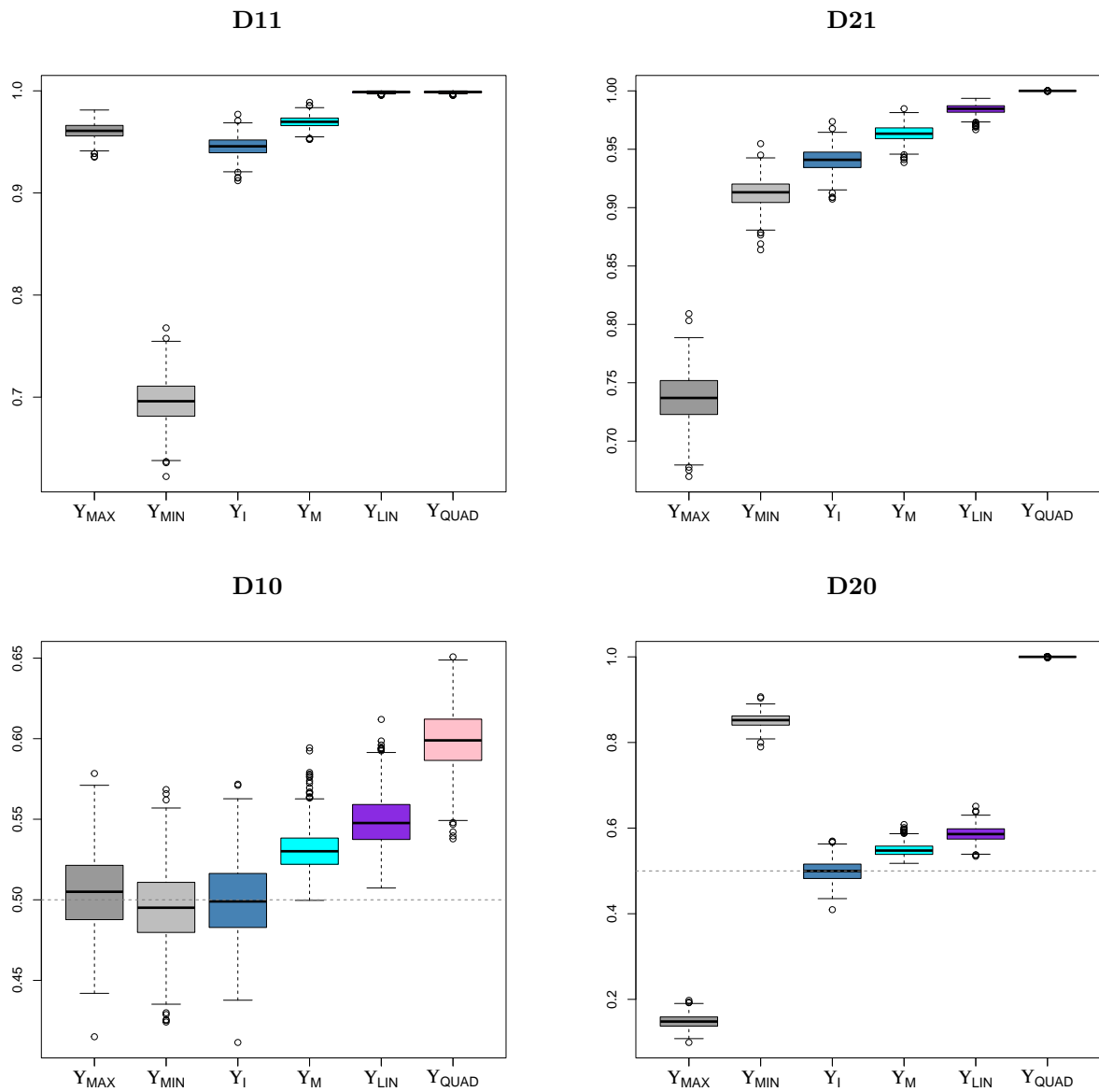


Figure 7: Boxplot of the estimators of the AUC under scheme **DIFF**. The horizontal dashed line, when appearing, indicates 0.5.

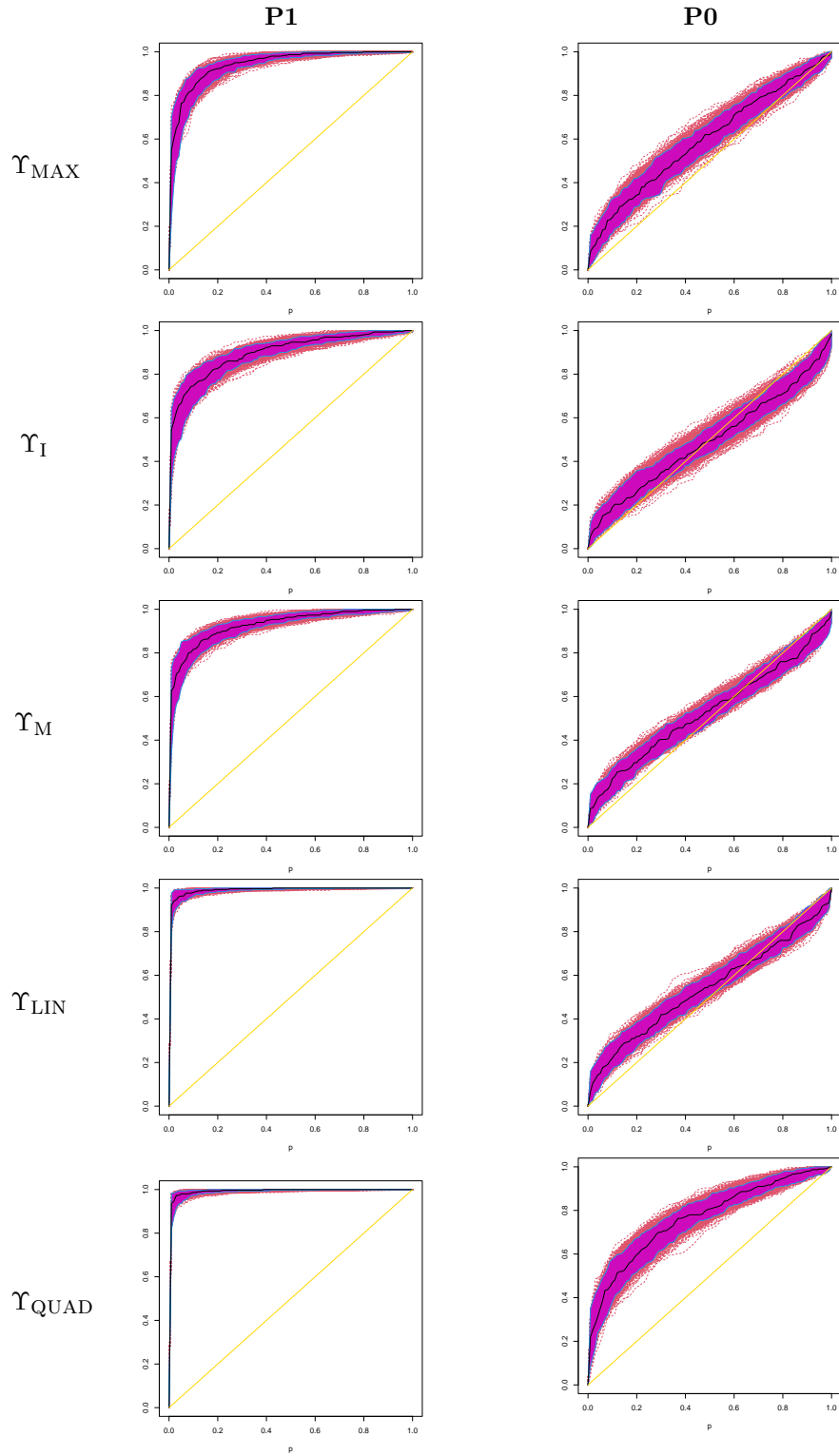


Figure 8: Functional boxplot of the estimators  $\widehat{\text{ROC}}$  under scenario **PROP** with  $\rho = 2$  for the Brownian motion setting. Rows correspond to discriminating indexes, while columns to  $\mu_D(t) = 2 \sin(\pi, t)$  and  $\mu_D = 0$ .

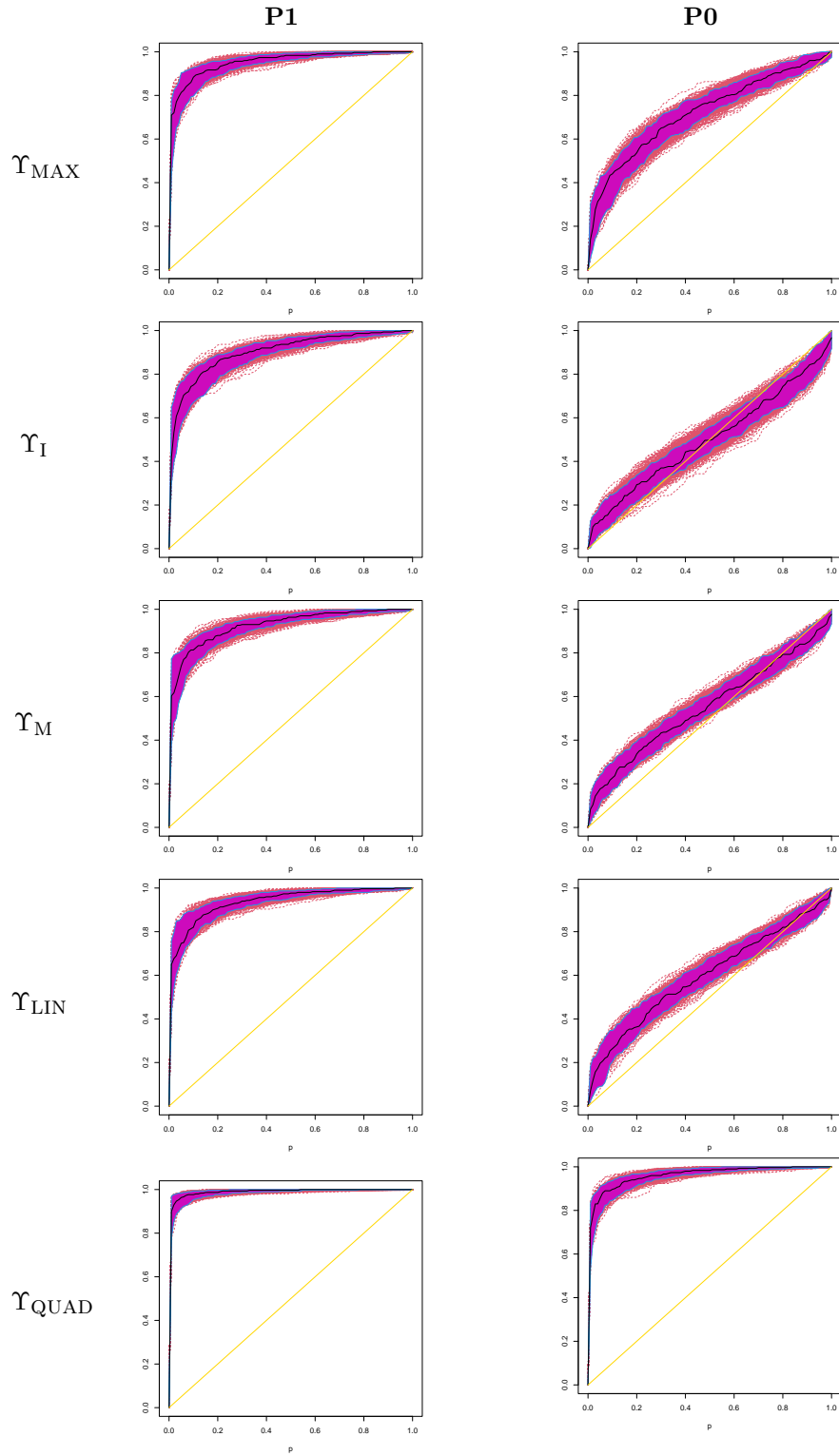


Figure 9: Functional boxplot of the estimators  $\widehat{\text{ROC}}$  under scenario **PROP** with  $\rho = 2$  for the Exponential Variogram process. Rows correspond to discriminating indexes, while columns to  $\mu_D(t) = 2 \sin(\pi, t)$  and  $\mu_D = 0$ .

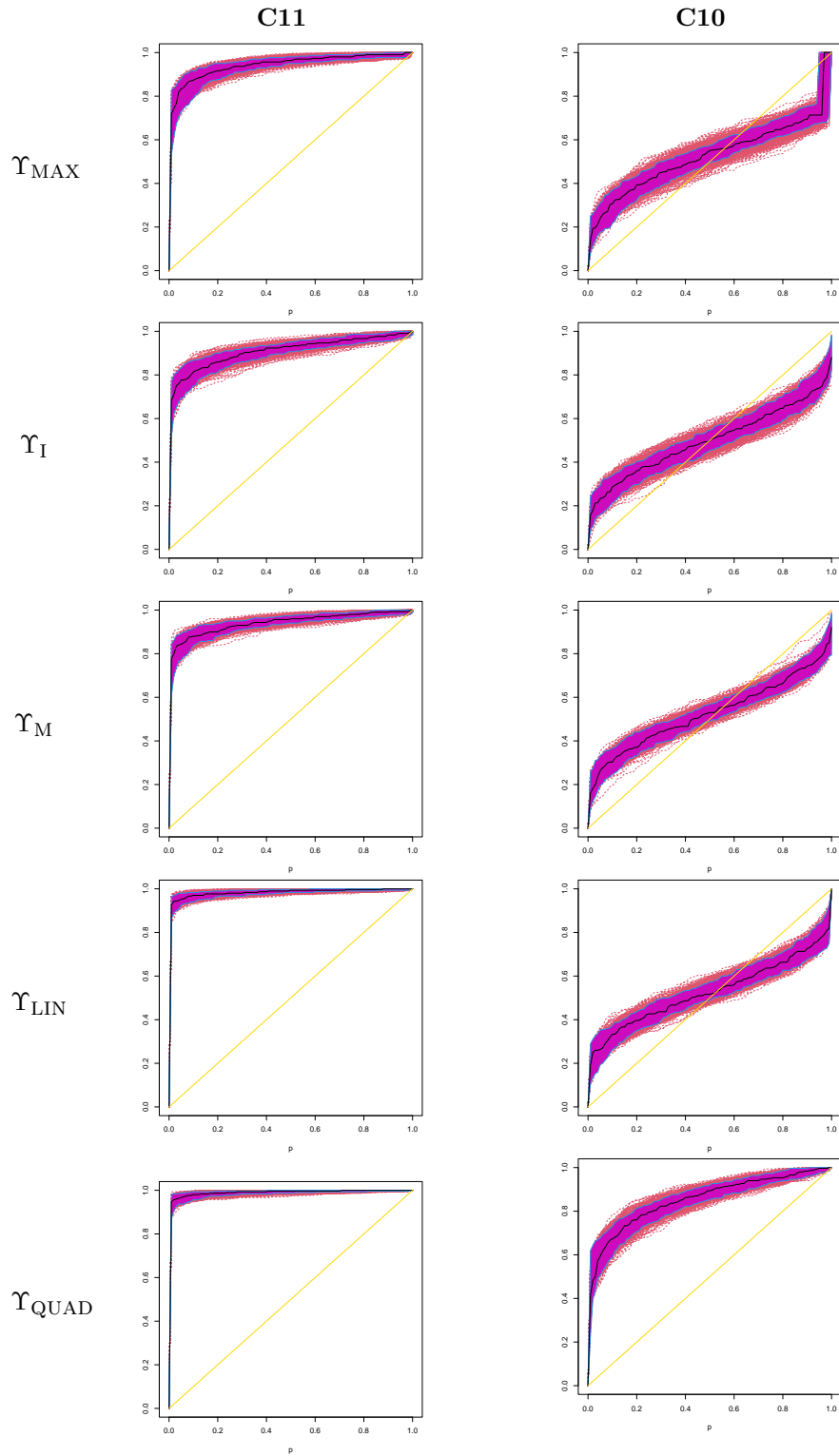


Figure 10: Functional boxplot of the estimators  $\widehat{\text{ROC}}$  under a FCPC model with  $\lambda_{D,1} = 2$ ,  $\lambda_{D,2} = 0.3$  and  $\lambda_{D,3} = 0.05$ . Rows correspond to discriminating indexes, while columns to  $\mu_D(t) = 2 \sin(\pi, t)$  and  $\mu_D = 0$ .

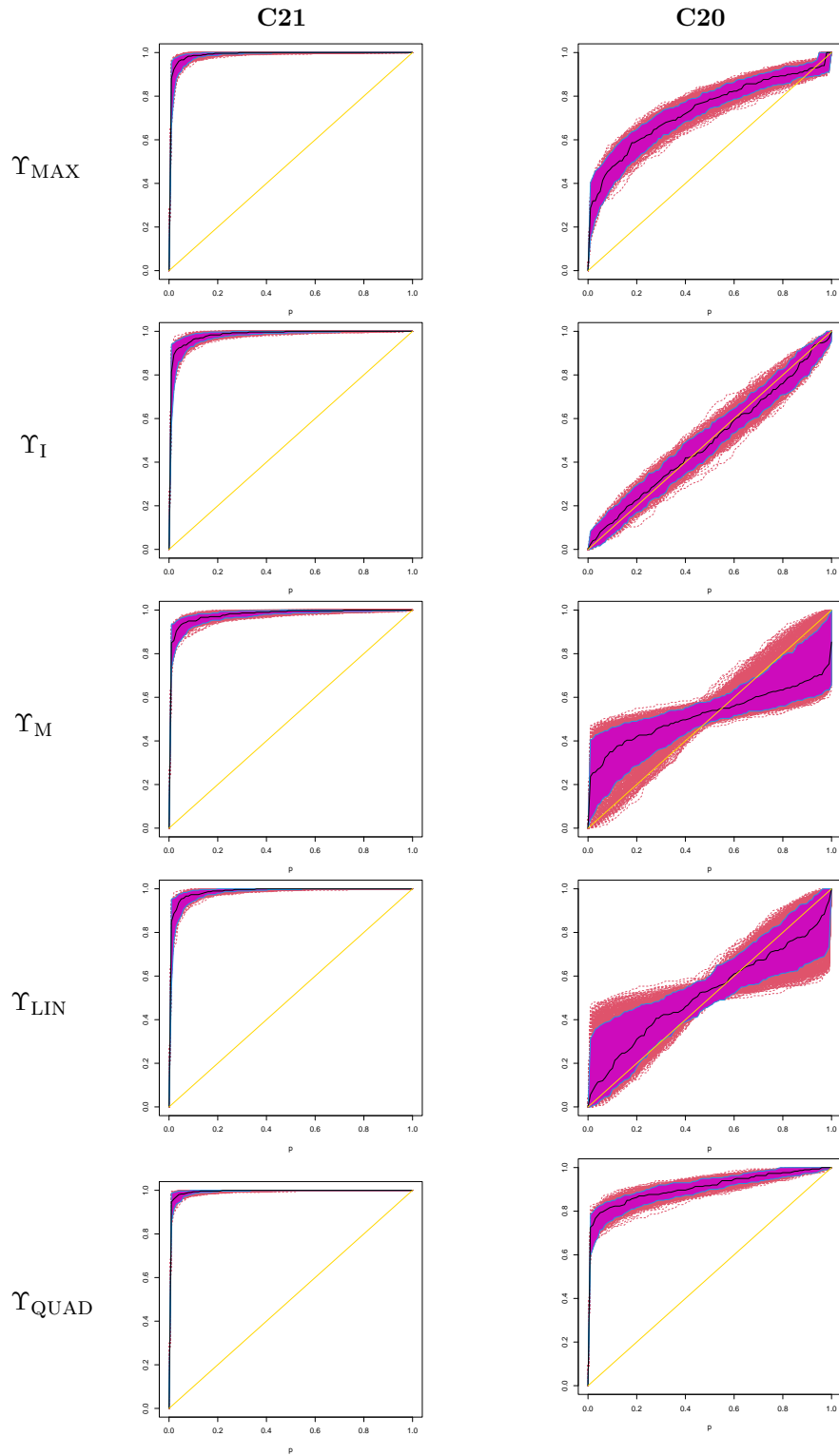


Figure 11: Functional boxplot of the estimators  $\widehat{ROC}$  under a FCPC model with  $\lambda_{D,1} = 0.3$ ,  $\lambda_{D,2} = 2$  and  $\lambda_{D,3} = 0.05$ . Rows correspond to discriminating indexes, while columns to  $\mu_D(t) = 2 \sin(\pi, t)$  and  $\mu_D = 0$ .

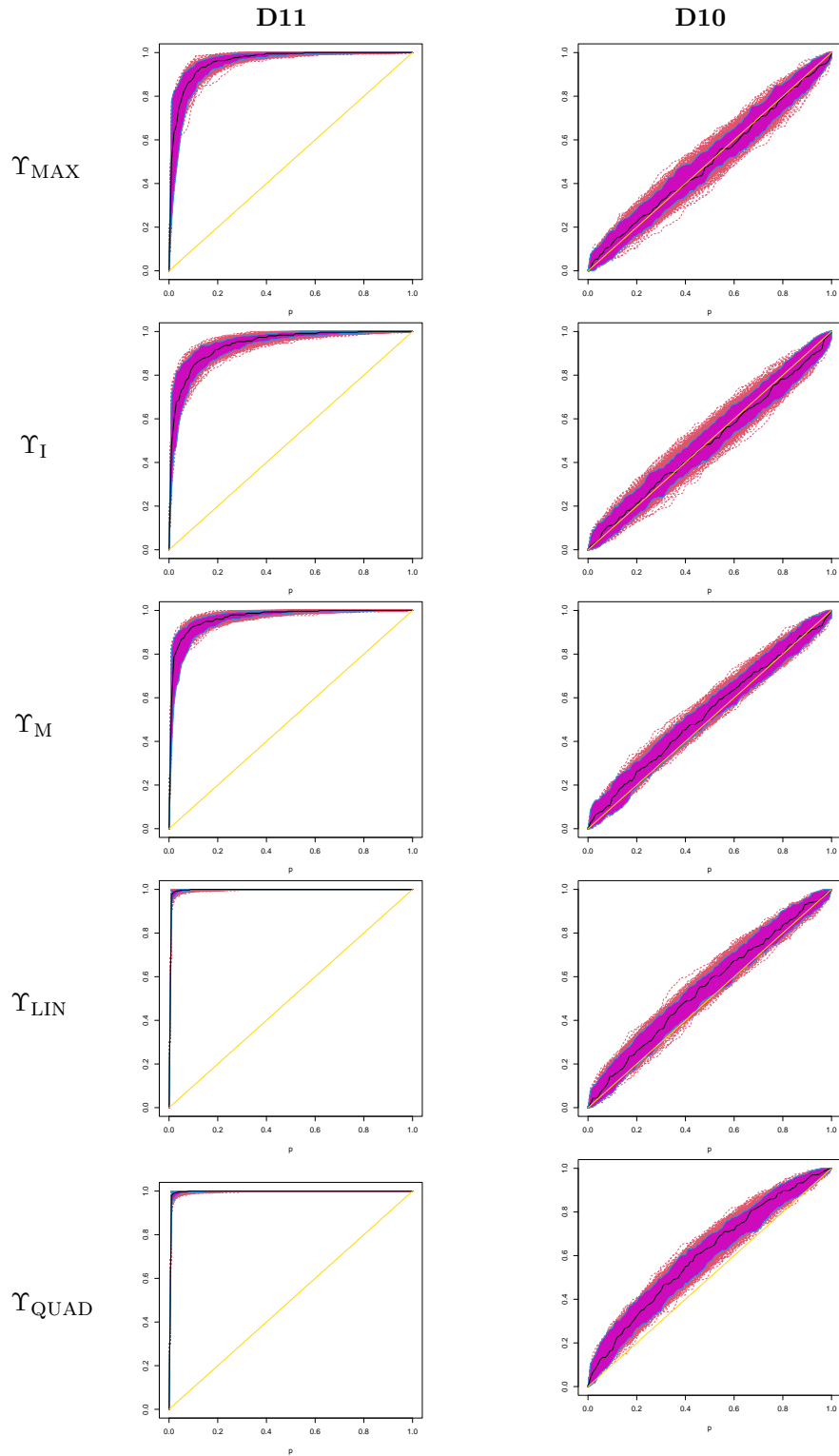


Figure 12: Functional boxplot of the estimators  $\widehat{\text{ROC}}$  under scheme **D1**. Rows correspond to discriminating indexes, while columns to  $\mu_D(t) = 2 \sin(\pi, t)$  and  $\mu_D = 0$ .

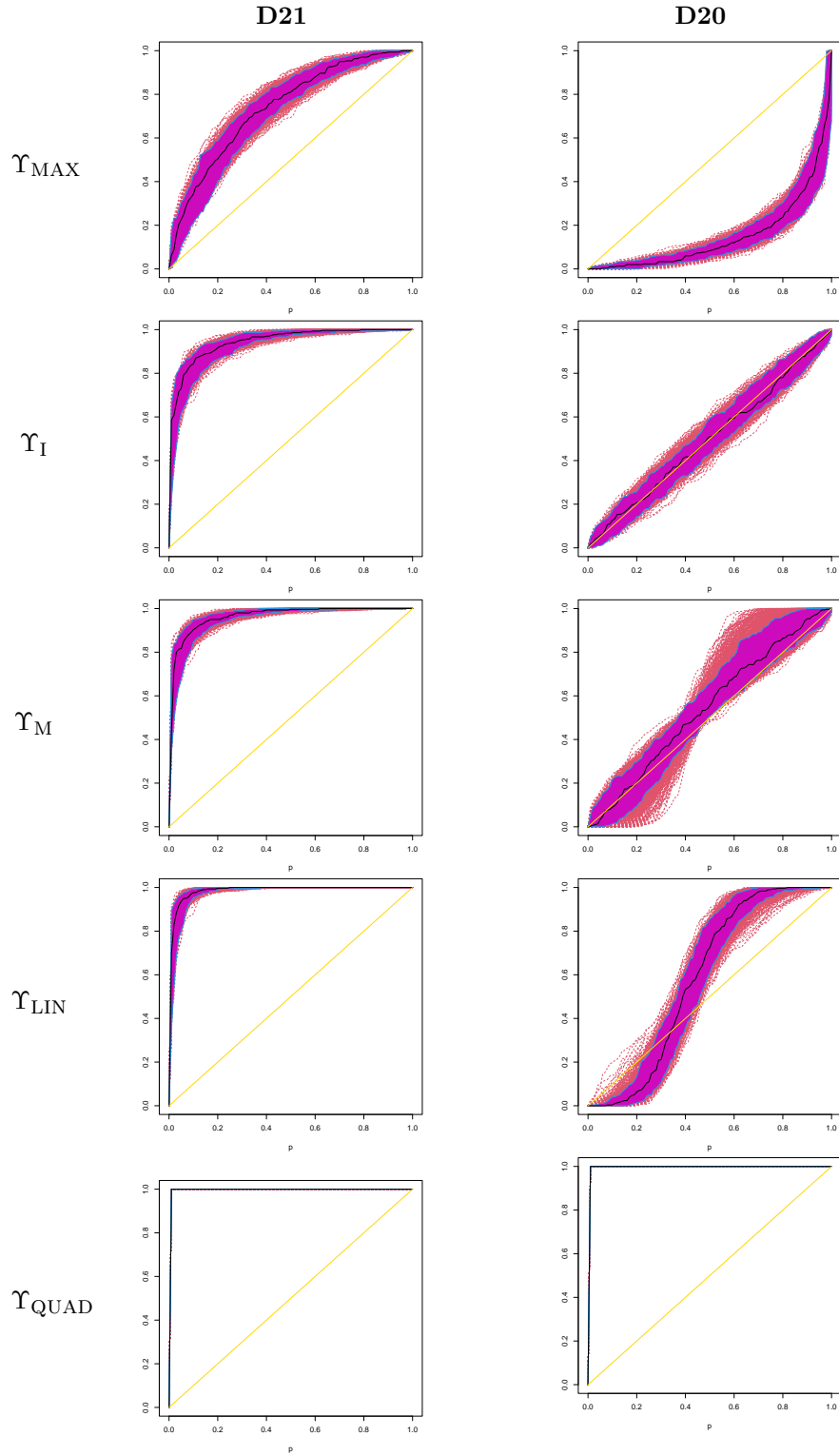


Figure 13: Functional boxplot of the estimators  $\widehat{ROC}$  under scheme **D2**. Rows correspond to discriminating indexes, while columns to  $\mu_D(t) = 2 \sin(\pi, t)$  and  $\mu_D = 0$ .

## 5.2 Numerical results for unbalanced designs

In this Section, we report the results of a numerical study conducted to evaluate the effect of unbalanced sample sizes. To consider a framework similar to the cardiotoxicity data set, we chose  $n_D = 30$  and  $n_H = 250$  under a proportional model with  $\rho = 2$ . Table 4 displays the mean and standard deviations of the AUC estimators, while Figures 14 and 15 display the functional boxplots corresponding to the estimates of the ROC. The obtained results reveal that, as for the situation where the two samples have the same size, the quadratic rule  $\Upsilon_{\text{QUAD}}$  outperforms the other competitors, even when this setting is not so harmful for the linear rule as the one where the covariance operators follow a functional common principal component model. This suggests that the quadratic rule should be taken into account in frameworks where equality of the covariance operators may be doubtful.

$\rho$		$\Upsilon_{\text{MAX}}$	$\Upsilon_{\text{MIN}}$	$\Upsilon_{\text{I}}$	$\Upsilon_{\text{M}}$	$\Upsilon_{\text{LIN}}$	$\Upsilon_{\text{QUAD}}$	$\Upsilon_{\text{MAX}}$	$\Upsilon_{\text{MIN}}$	$\Upsilon_{\text{I}}$	$\Upsilon_{\text{M}}$	$\Upsilon_{\text{LIN}}$	$\Upsilon_{\text{QUAD}}$
		<b>P1</b>						<b>P0</b>					
		Brownian Motion											
2	Mean	0.9435	0.6187	0.8965	0.9330	<i>0.9937</i>	<b>0.9951</b>	0.5986	0.4031	0.5005	0.5816	<i>0.6216</i>	<b>0.7917</b>
	SD	0.0212	0.0655	0.0346	0.0235	0.0067	0.0057	0.0585	0.0581	0.0635	0.0370	0.0458	0.0462
		Exponential Variogram											
2	Mean	0.9521	0.5520	0.9011	0.9295	<i>0.9683</i>	<b>0.9988</b>	0.7193	0.2828	0.5006	0.6518	<i>0.7670</i>	<b>0.9943</b>
	SD	0.0223	0.0658	0.0342	0.0274	0.0173	0.0017	0.0557	0.0546	0.0637	0.0363	0.0402	0.0052

Table 4: Mean and standard deviation of the  $\widehat{\text{AUC}}$ , under scenario **PROP**, that is, under a proportional model  $\gamma_D(t, s) = \rho \gamma_H(t, s)$  with equal (**P0**) or different mean functions (**P1**,  $\mu_H(t) = 0$  and  $\mu_D(t) = 2 \sin(\pi, t)$ ). In all cases,  $n_H = 250$  and  $n_D = 30$ .



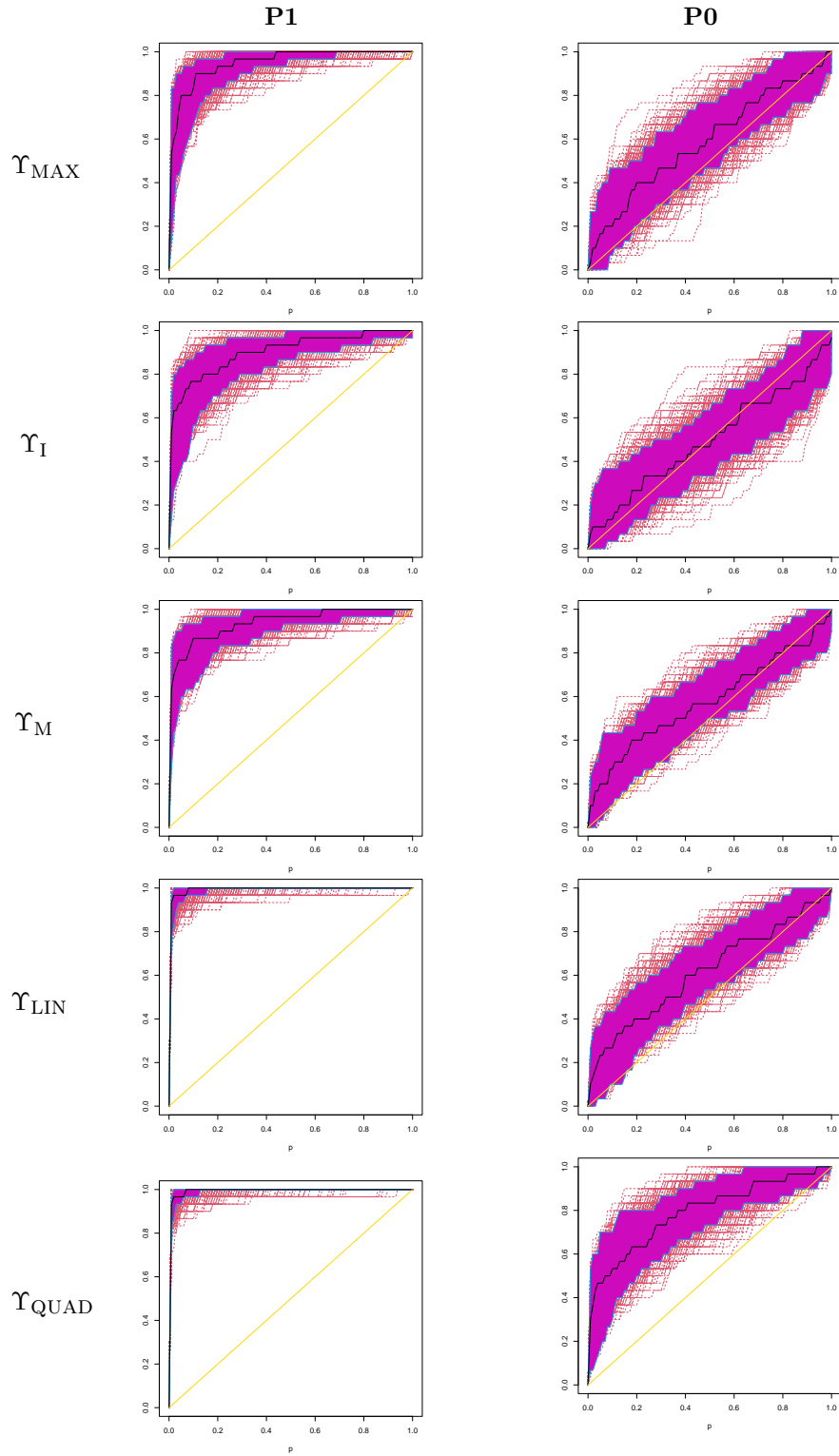


Figure 14: Functional boxplot of the estimators  $\widehat{\text{ROC}}$  under scenario **PROP** with  $\rho = 2$  for the Brownian motion setting. Rows correspond to discriminating indexes, while columns to  $\mu_D(t) = 2 \sin(\pi, t)$  and  $\mu_D = 0$ . The sample sizes are  $n_D = 30$  and  $n_H = 250$ .

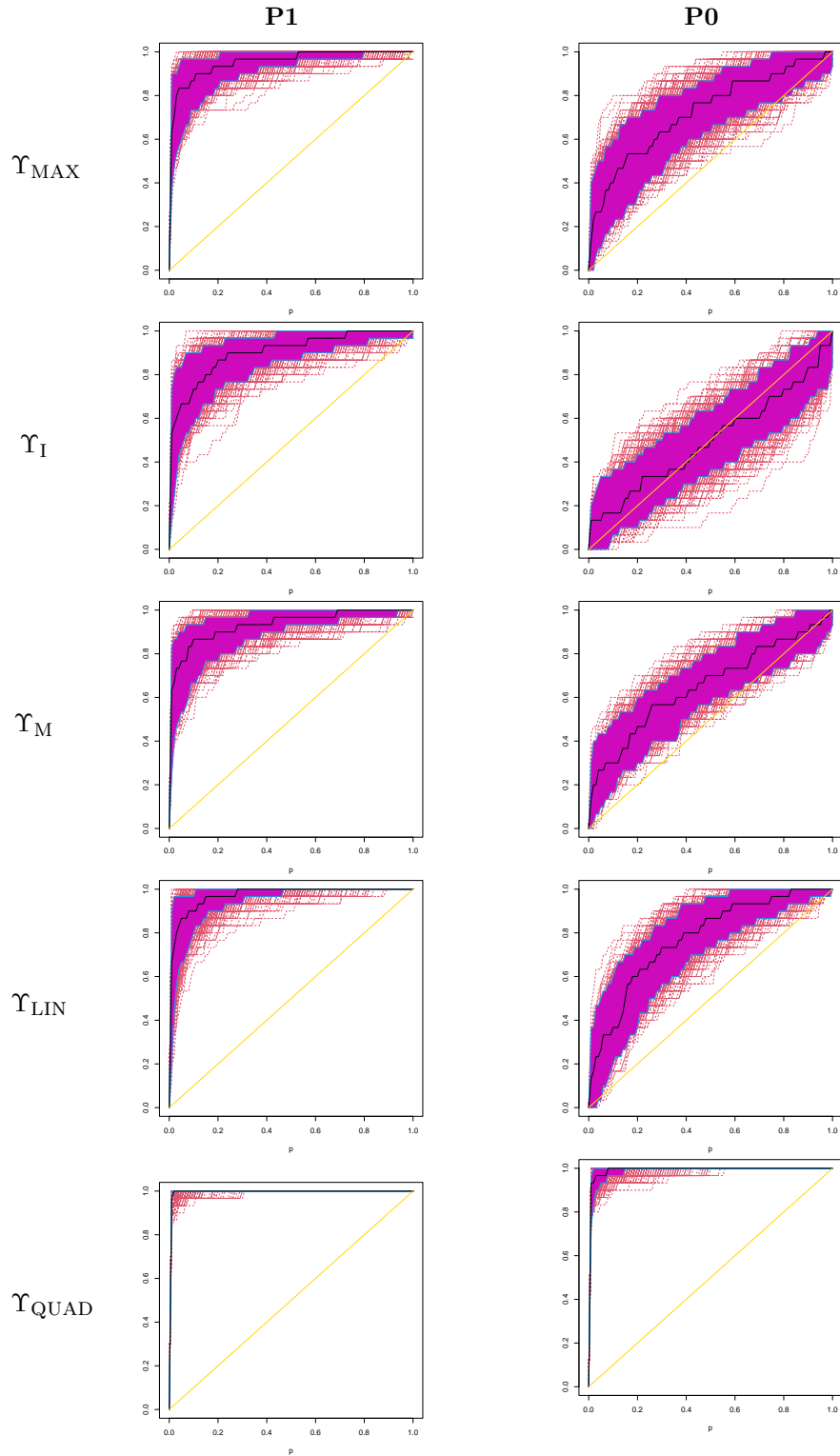


Figure 15: Functional boxplot of the estimators  $\widehat{ROC}$  under scenario **PROP** with  $\rho = 2$  for the Exponential Variogram process. Rows correspond to discriminating indexes, while columns to  $\mu_D(t) = 2 \sin(\pi, t)$  and  $\mu_D = 0$ . The sample sizes are  $n_D = 30$  and  $n_H = 250$ .

## 6 Real dataset analysis

We illustrate the application of the developed methodology to a real dataset reported in [Piñeiro-Lamas et al. \(2023\)](#) related to the study of cardiotoxicity in breast cancer patients mentioned in the Introduction.

Breast cancers related to high levels of the protein human epidermal growth factor receptor 2 (HER2) are much more likely to respond to treatments with drugs that target the HER2 protein. In fact, therapies that aim specifically HER2 have a strong anti-tumoral effect, improving the overall response of the patient and therefore, the survival expectancy. However, this kind of therapies may have side effects such as cardiotoxicity. In this context, the detection of the cancer therapy-related cardiac dysfunction (CTRCD) is relevant with respect to the prognosis and hence, it is recommended to follow-up the appearance of CTRCD through cardiac imaging tests, among other clinical tests. The availability of good markers to predict CTRCD is important to prevent cardiac problems. The Tissue Doppler Imaging (TDI) is an echocardiographic technique that shows the velocity of myocardial motion. It may be helpful to early identify CTRCD if a study of the heart condition is performed before treatment. TDI shows velocity as a function of time, thus it may be preprocessed to obtain a functional datum, see [Piñeiro-Lamas et al. \(2023\)](#) for more details.

The data correspond to 270 women diagnosed with HER2+ breast cancer, 27 of them suffer from CTRCD. For each patient the cycle extracted from the TDI discretized in 1001 equispaced points in the interval  $[0,1]$  is registered together with their CTRCD status. Figure 16 displays the standardized cycles for the 270 patients, gray curves correspond to patients without CTRCD (CTRCD= 0) and aquamarine ones to women with CTRCD (CTRCD= 1). The mean of each group is also plotted, the line in black corresponds to patients without CTRCD and the gold one to those with CTRCD= 1. At a first glance, the two groups look different since the cycles of patients without CTRCD are more spread, while the data of women that experienced CTRCD are more concentrated in the central area. Besides, the means of the two groups are similar, except for cycle values between 0.4 and 0.8.

To have a deeper insight of the cycles in each status of CTRCD, in Figure 17 we display the functional boxplot of each group. No outlying cycles were detected in either group.

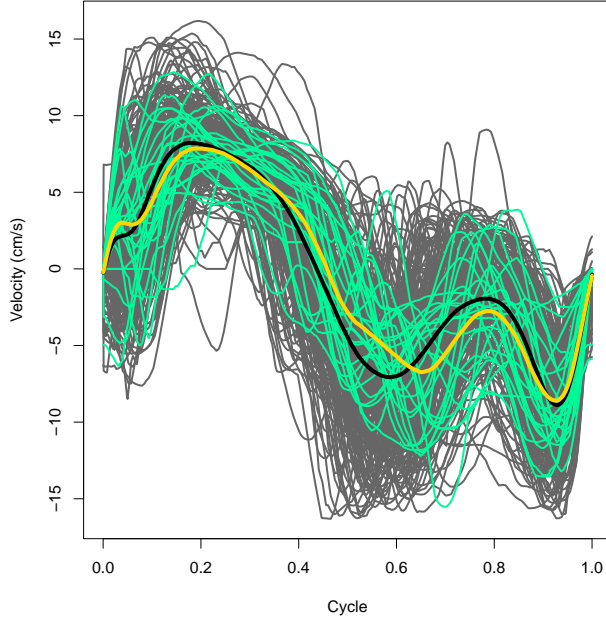


Figure 16: Cardiotoxicity data. Cycles of 270 patients during the follow-up. The cycles of patients with  $\text{CTRCD}=0$  are displayed as gray lines, while those with  $\text{CTRCD}=1$  are represented in in aquamarine. The lines in black and gold correspond to the mean of  $\text{CTRCD}=0$  and  $\text{CTRCD}=1$ , respectively.

In order to assess the performance of the functional biomarker to distinguish between the two categories of  $\text{CTRCD}$ , we apply the discriminating indexes described in the previous sections. We computed the indexes based on the minimum ( $\Upsilon_{\text{MIN}}$ ), the maximum ( $\Upsilon_{\text{MAX}}$ ), the integral ( $\Upsilon_{\text{I}}$ ), the difference of means ( $\Upsilon_{\text{M}}$ ), and the linear ( $\Upsilon_{\text{LIN}}$ ) and the quadratic ( $\Upsilon_{\text{QUAD}}$ ) criteria taking the number of components that explain at least 95% of the variability, which in this data is attained for  $k = 11$ . Table 5 collects the AUC for each method. In Figure 18 the estimates of the ROC curve with AUC greater or equal to 0.65 are depicted. The estimator obtained from the quadratic method is plotted in black, in magenta the one corresponding to the linear rule, in green the estimate based on the difference of means and in blue that related to the minimum. It is evident from this figure that the better performance is achieved for the quadratic method. The better discriminating capability of the quadratic method is in some sense expectable due to the particular structure of the data, which makes difficult to distinguish the groups just taking into account either the minimum or the maximum or any linear rule.

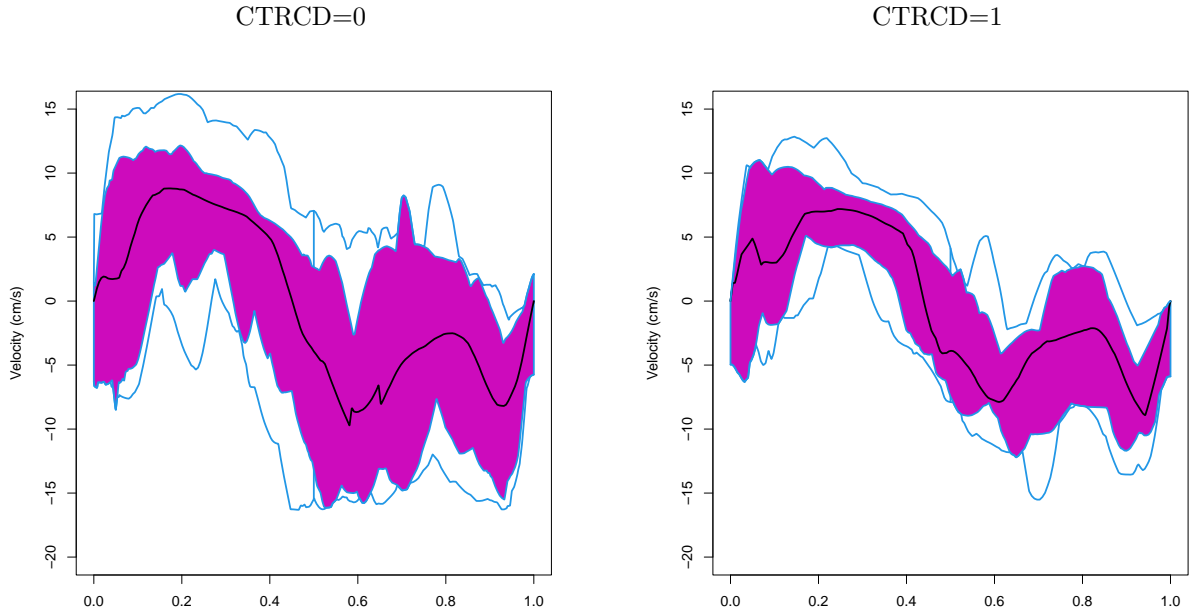


Figure 17: Cardiotoxicity data. Left panel corresponds to the functional boxplot of the cycles of patients without CTRCD, while the right one to women with CTRCD.

$\Upsilon_{\text{MAX}}$	$\Upsilon_{\text{MIN}}$	$\Upsilon_{\text{I}}$	$\Upsilon_{\text{M}}$	$\Upsilon_{\text{LIN}}$	$\Upsilon_{\text{QUAD}}$
0.4547	0.6770	0.5328	0.6819	0.7072	0.8877

Table 5: Cardiotoxicity data. AUC of each method.

## 7 Final Comments

In this paper, in order to construct a suitable ROC curve, we address the problem of defining proper univariate indexes when functional biomarkers are used to distinguish between two populations. The defined indexes allow to construct a ROC curve to measure its discriminating capability. In particular, we introduce a linear index with the property of maximizing the AUC, when both populations have the same covariance operator and, in order to estimate it, we circumvent the curse of dimensionality by using a sieve or penalized approach. The situation of different covariance structures is also contemplated by means of a quadratic rule.

Consistency results for the estimators of the ROC curve and its related summary measures are derived for both linear and quadratic discriminating indexes, under general assumptions. The results of our numerical experiments illustrate the advantages of using a quadratic rule in

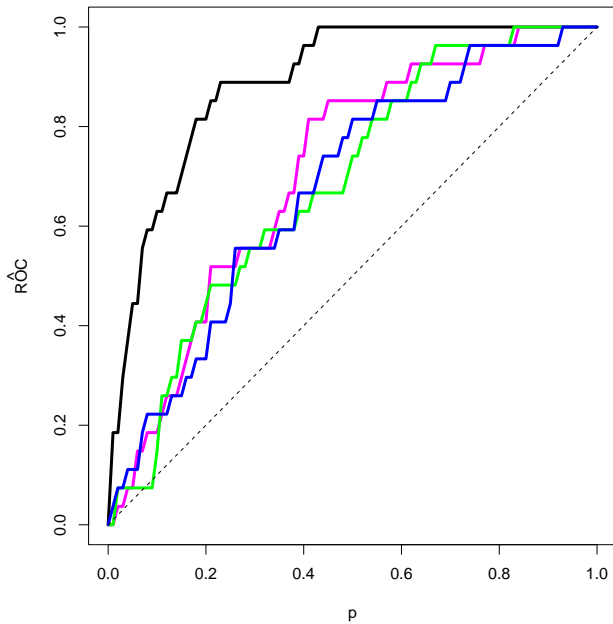


Figure 18: Cardiotoxicity data. Estimated ROC curves with  $AUC \geq 0.65$ . The black, magenta, green and blue lines correspond to the estimators related to the quadratic method, the linear rule, the procedure based on the difference of means and the one based on the minimum, respectively.

presence of different covariance operators. The application of our proposals to a real data set confirms that, when differences between populations arise in covariances more than between mean, as revealed in Figure 16, the quadratic index outperforms the linear one.

## 8 Appendix: Proofs

### 8.1 Proof of the results in Section 2.2

*Proof of (3).* To derive (3), first note that the value  $c$  maximizing  $\Delta_{\beta}(c)$  equals

$$c_{\beta} = \frac{\beta^T(\boldsymbol{\mu}_D + \boldsymbol{\mu}_H)}{2}$$

giving the following expression for the Youden index

$$\begin{aligned} \text{YI}(\boldsymbol{\beta}) &= \left| \Phi \left( \frac{\boldsymbol{\beta}^T (\boldsymbol{\mu}_H - \boldsymbol{\mu}_D)}{2\sqrt{\boldsymbol{\beta}^T \boldsymbol{\Sigma} \boldsymbol{\beta}}} \right) - \Phi \left( \frac{\boldsymbol{\beta}^T (\boldsymbol{\mu}_D - \boldsymbol{\mu}_H)}{2\sqrt{\boldsymbol{\beta}^T \boldsymbol{\Sigma} \boldsymbol{\beta}}} \right) \right| = \left| 1 - 2 \Phi \left( \frac{\boldsymbol{\beta}^T (\boldsymbol{\mu}_D - \boldsymbol{\mu}_H)}{2\sqrt{\boldsymbol{\beta}^T \boldsymbol{\Sigma} \boldsymbol{\beta}}} \right) \right| \\ &= \left| 1 - 2 \Phi \left( \frac{1}{\sqrt{2}} L(\boldsymbol{\beta}) \right) \right|. \end{aligned}$$

To simplify the notation let  $\sigma_\beta^2 = \boldsymbol{\beta}^T \boldsymbol{\Sigma} \boldsymbol{\beta}$  and  $\boldsymbol{\mu} = (\boldsymbol{\mu}_D - \boldsymbol{\mu}_H)/2$ . Then,

$$\text{YI}(\boldsymbol{\beta}) = \left| 1 - 2 \Phi \left( \frac{\boldsymbol{\beta}^T \boldsymbol{\mu}}{\sigma_\beta} \right) \right|.$$

Taking into account that multiplying  $\boldsymbol{\beta}$  by a constant does not change the value of the Youden index, to maximize it, we can search for the maximum of  $\text{YI}^2(\boldsymbol{\beta})$  under the constraint that  $\sigma_\beta^2 = 1$ . Let

$$H(\boldsymbol{\beta}) = \{1 - 2 \Phi(\boldsymbol{\beta}^T \boldsymbol{\mu})\}^2 + \lambda(\sigma_\beta^2 - 1).$$

Then, if  $\varphi = \Phi'$ , we get that

$$\frac{\partial H}{\partial \boldsymbol{\beta}} = -4 \{1 - 2 \Phi(\boldsymbol{\beta}^T \boldsymbol{\mu})\} \varphi(\boldsymbol{\beta}^T \boldsymbol{\mu}) \boldsymbol{\mu} + 2\lambda \boldsymbol{\Sigma} \boldsymbol{\beta}. \quad (15)$$

Multiplying (15) by  $\boldsymbol{\beta}^T$  and using that the value maximizing  $H(\boldsymbol{\beta})$  has null gradient and that  $\sigma_\beta^2 = 1$ , we obtain that

$$\begin{aligned} 0 &= -4 \{1 - 2 \Phi(\boldsymbol{\beta}^T \boldsymbol{\mu})\} \varphi(\boldsymbol{\beta}^T \boldsymbol{\mu}) \boldsymbol{\beta}^T \boldsymbol{\mu} + 2\lambda \boldsymbol{\beta}^T \boldsymbol{\Sigma} \boldsymbol{\beta} \\ &= -4 \{1 - 2 \Phi(\boldsymbol{\beta}^T \boldsymbol{\mu})\} \varphi(\boldsymbol{\beta}^T \boldsymbol{\mu}) \boldsymbol{\beta}^T \boldsymbol{\mu} + 2\lambda, \end{aligned}$$

which entails that

$$2\lambda = 4 \{1 - 2 \Phi(\boldsymbol{\beta}^T \boldsymbol{\mu})\} \varphi(\boldsymbol{\beta}^T \boldsymbol{\mu}) \boldsymbol{\beta}^T \boldsymbol{\mu}. \quad (16)$$

Therefore, if  $\boldsymbol{\beta}^T \boldsymbol{\mu} = 0$ , we have that  $\lambda = 0$ ,  $\mathbf{0} = \partial H / \partial \boldsymbol{\beta}$  and  $H(\boldsymbol{\beta}) = 0$  meaning that the maximum is not reached in directions orthogonal to  $\boldsymbol{\mu}$ .

Assume that  $\boldsymbol{\beta}^T \boldsymbol{\mu} \neq 0$  and let  $\nu_\beta = 4 \{1 - 2 \Phi(\boldsymbol{\beta}^T \boldsymbol{\mu})\} \varphi(\boldsymbol{\beta}^T \boldsymbol{\mu}) \neq 0$ . Using (16), we conclude that  $2\lambda = \nu_\beta \boldsymbol{\beta}^T \boldsymbol{\mu}$ . Besides, taking into account that at any critical point  $\partial H / \partial \boldsymbol{\beta} = \mathbf{0}$ , from (15) we conclude that  $2\lambda \boldsymbol{\Sigma} \boldsymbol{\beta} = 4 \{1 - 2 \Phi(\boldsymbol{\beta}^T \boldsymbol{\mu})\} \varphi(\boldsymbol{\beta}^T \boldsymbol{\mu}) \boldsymbol{\mu} = \nu_\beta \boldsymbol{\mu}$ , so

$$\nu_\beta \boldsymbol{\beta}^T \boldsymbol{\mu} \boldsymbol{\Sigma} \boldsymbol{\beta} = \nu_\beta \boldsymbol{\mu},$$

or equivalently,  $(\boldsymbol{\beta}^T \boldsymbol{\mu}) \boldsymbol{\Sigma} \boldsymbol{\beta} = \boldsymbol{\mu}$ . Denoting  $a_\beta = \boldsymbol{\beta}^T \boldsymbol{\mu} \neq 0$ , we have

$$\boldsymbol{\beta} = \boldsymbol{\Sigma}^{-1} \boldsymbol{\mu} \frac{1}{a_\beta},$$

which leads to  $a_\beta^2 = \boldsymbol{\mu}^T \boldsymbol{\Sigma}^{-1} \boldsymbol{\mu}$  and  $\boldsymbol{\beta} = \boldsymbol{\Sigma}^{-1} \boldsymbol{\mu} / \sqrt{\boldsymbol{\mu}^T \boldsymbol{\Sigma}^{-1} \boldsymbol{\mu}}$ , concluding the proof. ■

## 8.2 Proof of the results in Section 3

*Proof of Lemma 3.1.* a) Note that as in the multivariate setting

$$\begin{aligned}
\text{Cov}(\langle \beta, X \rangle, G) &= \mathbb{E}(G \langle \beta, X \rangle) - \mathbb{E}\langle \beta, X \rangle \mathbb{E}G = \mathbb{E}\{G \mathbb{E}(\langle \beta, X \rangle | G)\} - \pi_D \mathbb{E}\{\mathbb{E}(\langle \beta, X \rangle | G)\} \\
&= \pi_D \mathbb{E}(\langle \beta, X \rangle | G = 1) - \pi_D \{\pi_D \mathbb{E}(\langle \beta, X \rangle | G = 1) + \pi_H \mathbb{E}(\langle \beta, X \rangle | G = 0)\} \\
&= \pi_D \{\mathbb{E}(\langle \beta, X_D \rangle) - [\pi_D \mathbb{E}(\langle \beta, X_D \rangle) + \pi_H \mathbb{E}(\langle \beta, X_H \rangle)]\} \\
&= \pi_D \{\langle \beta, \mu_D \rangle - [\pi_D \langle \beta, \mu_D \rangle + \pi_H \langle \beta, \mu_H \rangle]\} = \pi_D \{\pi_H \langle \beta, \mu_D \rangle - \pi_H \langle \beta, \mu_H \rangle\} \\
&= \pi_D \pi_H \langle \beta, \mu_D - \mu_H \rangle, \tag{17}
\end{aligned}$$

while

$$\begin{aligned}
\text{VAR}(\langle \beta, X \rangle) &= \mathbb{E}(\langle \beta, X \rangle^2) - \{\mathbb{E}\langle \beta, X \rangle\}^2 = \mathbb{E}(\langle \beta, X \rangle^2) - \{\pi_D \langle \beta, \mu_D \rangle + \pi_H \langle \beta, \mu_H \rangle\}^2 \\
&= \mathbb{E}\{\mathbb{E}(\langle \beta, X \rangle^2 | G)\} - \{\pi_D \langle \beta, \mu_D \rangle + \pi_H \langle \beta, \mu_H \rangle\}^2 \\
&= \{\pi_D \mathbb{E}(\langle \beta, X_D \rangle^2) + \pi_H \mathbb{E}(\langle \beta, X_H \rangle^2)\} - \{\pi_D \langle \beta, \mu_D \rangle + \pi_H \langle \beta, \mu_H \rangle\}^2 \\
&= \pi_D [\langle \beta, \Gamma_D \beta \rangle + \langle \beta, \mu_D \rangle^2] + \pi_H [\langle \beta, \Gamma_H \beta \rangle + \langle \beta, \mu_H \rangle^2] \\
&\quad - \{\pi_D^2 \langle \beta, \mu_D \rangle^2 + \pi_H^2 \langle \beta, \mu_H \rangle^2 + 2\pi_D \pi_H \langle \beta, \mu_D \rangle \langle \beta, \mu_H \rangle\} \\
&= \langle \beta, \Gamma_{\text{POOL}} \beta \rangle + \pi_D \pi_H \langle \beta, \mu_D \rangle^2 + \pi_D \pi_H \langle \beta, \mu_H \rangle^2 - 2\pi_D \pi_H \langle \beta, \mu_D \rangle \langle \beta, \mu_H \rangle.
\end{aligned}$$

Therefore,

$$\text{VAR}(\langle \beta, X \rangle) = \langle \beta, \Gamma_{\text{POOL}} \beta \rangle + \pi_D \pi_H \langle \beta, \mu_D - \mu_H \rangle^2,$$

which together with the fact that  $\text{VAR}(G) = \pi_D \pi_H$  entails that

$$\text{corr}(\langle \beta, X \rangle, G) = \frac{\pi_D \pi_H \langle \beta, \mu_D - \mu_H \rangle}{\{\pi_D \pi_H [\langle \beta, \Gamma_{\text{POOL}} \beta \rangle + \pi_D \pi_H \langle \beta, \mu_D - \mu_H \rangle^2]\}^{1/2}} = \frac{\pi_D^{1/2} \pi_H^{1/2} L_{\text{POOL}}(\beta)}{\{[1 + L_{\text{POOL}}^2(\beta)]\}^{1/2}},$$

concluding the proof of (a).

b) Follows immediately noting that  $\Gamma_{\text{POOL}} = \Gamma$  when  $\pi_D = 1/2$  or when  $\Gamma_H = \Gamma_D$ , since  $\pi_D + \pi_H = 1$  and the analogy between maximizing the AUC which corresponds to maximizing  $L(\beta)$  and that of maximizing  $\text{corr}(\langle \beta, X \rangle, Z)$ , which corresponds to  $L_{\text{POOL}}(\beta)$ .  $\blacksquare$

*Proof of Proposition 3.2.* Analogously to  $\mathcal{R}(\Gamma)$ , define

$$\mathcal{R}(\Gamma^{1/2}) = \left\{ y \in \mathcal{H} : \sum_{\ell \geq 1} \frac{1}{\lambda_\ell} \langle y, \phi_\ell \rangle^2 < \infty \right\},$$



and the inverse of  $\Gamma^{1/2}$ , which is well defined over  $\mathcal{R}(\Gamma^{1/2})$ , as

$$\Gamma^{-1/2}(y) = \sum_{\ell \geq 1} \frac{1}{\sqrt{\lambda_\ell}} \langle y, \phi_\ell \rangle \phi_\ell.$$

The fact that  $\lambda_\ell \rightarrow 0$  as  $\ell \rightarrow \infty$  entails that for  $\ell$  large enough  $\lambda_\ell^2 < \lambda_\ell$ , so taking into account that  $\mu_D - \mu_H \in \mathcal{R}(\Gamma)$ , we get that  $\mu_D - \mu_H \in \mathcal{R}(\Gamma^{1/2})$ .

Let  $R = \Gamma^{-1/2} \Gamma_{XG} / \sqrt{\pi_D \pi_H} : \mathbb{R} \rightarrow L^2(0, 1)$  with  $\Gamma_{XG}$  the covariance operator between  $X$  and  $G$ , that is, the operator  $\Gamma_{XG} : \mathbb{R} \rightarrow \mathcal{H}$  and is such that for any  $a \in \mathbb{R}$ ,  $\text{COV}(\langle u, X \rangle, aG) = \langle u, \Gamma_{XG}(a) \rangle$ . Denoting  $\gamma_{XG} = \Gamma_{XG}(1)$  we have that  $\text{COV}(\langle u, X \rangle, G) = \langle u, \gamma_{XG} \rangle$ . Analogous arguments to those considered in Theorem 4.8 of [He et al. \(2003\)](#) allow to show that the value  $\beta_0$  maximizing  $\text{corr}^2(\langle \beta, X \rangle, G)$  (respectively, the AUC) equals  $\beta_0 = \Gamma^{-1/2} \psi_0$  where  $\psi_0$  is the eigenfunction of the operator

$$R_0 = R R^* : L^2(0, 1) \rightarrow L^2(0, 1)$$

related to its largest eigenvalue, where  $R^*$  stands for the adjoint operator of  $R$ .

From (17), we get that  $\gamma_{XG} = \pi_D \pi_H (\mu_D - \mu_H)$ , then if  $\Delta_{DH} = \sqrt{\pi_D \pi_H} \Gamma^{-1/2} (\mu_D - \mu_H) \in \mathcal{H}$ , we get that  $Ra = a \Delta_{DH}$  and  $R_0 = \Delta_{DH} \{\Delta_{DH}\}^*$ . Note that  $R^* : L^2(0, 1) \rightarrow \mathbb{R}$  satisfies  $\langle u, R a \rangle = a R^* u$ , for any  $a \in \mathbb{R}$ ,  $u \in L^2(0, 1)$ , hence we have that

$$\langle u, R a \rangle = a \langle u, \Delta_{DH} \rangle = a \int_0^1 \Delta_{DH}(t) u(t) dt,$$

and  $R^*$  is the linear operator with representative  $\Delta_{DH}$ , i.e.,  $R^* u = \langle u, \Delta_{DH} \rangle$ . Hence,  $R_0$  has only one eigenvalue different from 0, since for any  $u \in \mathcal{H}$  orthogonal to  $\Delta_{DH}$ ,  $R_0 u = 0$  and  $R^* \Delta_{DH} = \|\Delta_{DH}\|^2$  meaning that

$$R_0 \Delta_{DH} = R \|\Delta_{DH}\|^2 = \|\Delta_{DH}\|^2 \Delta_{DH}.$$

Thus,  $\psi_0 = \Delta_{DH} / \|\Delta_{DH}\|$  and  $\beta_0 = \sqrt{\pi_D \pi_H} \Gamma^{-1} (\mu_D - \mu_H)$ , concluding the proof.  $\blacksquare$

*Proof of Proposition 3.3.* a) follows easily noting that  $A^* A \alpha = \sum_{\ell=1}^k \langle \alpha, \phi_\ell \rangle \phi_\ell$ ,  $\alpha^T \mathbf{x} = \langle A \alpha, AX \rangle$  and the fact that

$$\Gamma_j^{-1} y = \sum_{\ell \geq 1} \frac{1}{\lambda_{j,\ell}} \langle y, \phi_\ell \rangle \phi_\ell, \quad \text{for any } y \in \mathcal{R}(\Gamma_j), \quad (18)$$

which implies that  $A \Gamma_j^{-1} \mu_j = \Sigma_j^{-1} \mu_j$ .

b) Note that

$$\mathbf{x}^T \mathbf{\Lambda} \mathbf{x} = \sum_{\ell=1}^k \Lambda_{\ell} x_{\ell}^2 = \sum_{\ell=1}^k \Lambda_{\ell} \langle X, \phi_{\ell} \rangle^2 = \sum_{\ell=1}^k \frac{1}{\lambda_{D,\ell}} \langle X, \phi_{\ell} \rangle^2 - \sum_{\ell=1}^k \frac{1}{\lambda_{H,\ell}} \langle X, \phi_{\ell} \rangle^2.$$

Taking into account (18) and that from the definition of the linear operator  $A$ , we have that

$$A\Gamma_j^{-1}y = \left( \frac{\langle y, \phi_1 \rangle}{\lambda_{j,1}}, \dots, \frac{\langle y, \phi_k \rangle}{\lambda_{j,k}} \right)^T,$$

we easily obtain that, for any  $X \in \mathcal{R}(\Gamma_D^{1/2}) \cap \mathcal{R}(\Gamma_H^{1/2})$ ,

$$\sum_{\ell=1}^k \frac{1}{\lambda_{j,\ell}} \langle X, \phi_{\ell} \rangle^2 = \|A\Gamma_j^{-1}X\|^2.$$

The expression for  $\Upsilon(X)$  follows easily from the convergence of the series,  $\sum_{\ell \geq 1} \langle X, \phi_{\ell} \rangle^2 / \lambda_{j,\ell}$ , for  $j = D, H$ , and of the series  $\sum_{\ell \geq 1} \langle \alpha, \phi_{\ell} \rangle \langle X, \phi_{\ell} \rangle = \langle \alpha, X \rangle$  concluding the proof. ■

### 8.3 Proof of the results in Section 4

*Proof of Theorem 4.1.* From A3 and the continuity of the quantile function  $F_H^{-1} = F_{H,\Upsilon}^{-1} : [0, 1] \rightarrow \mathbb{R}$  when A1 holds, we get that for each  $0 < p < 1$ ,  $\widehat{F}_j^{-1}(p) - F_j^{-1}(p) \xrightarrow{a.s.} 0$ , therefore using that

$$\begin{aligned} |\widehat{\text{ROC}}(p) - \text{ROC}(p)| &= \left| \widehat{F}_D \left( \widehat{F}_H^{-1}(1-p) \right) - F_D \left( F_H^{-1}(1-p) \right) \right| \\ &\leq \left| \widehat{F}_D \left( \widehat{F}_H^{-1}(1-p) \right) - F_D \left( \widehat{F}_H^{-1}(1-p) \right) \right| + \left| F_D \left( \widehat{F}_H^{-1}(1-p) \right) - F_D \left( F_H^{-1}(1-p) \right) \right| \\ &\leq \left\| \widehat{F}_D - F_D \right\|_{\infty} + \left| F_D \left( \widehat{F}_H^{-1}(1-p) \right) - F_D \left( F_H^{-1}(1-p) \right) \right|, \end{aligned}$$

the continuity of  $F_D$  stated in assumption A2 and the uniform convergence required in A3 for  $j = D$ , we derive that  $\widehat{\text{ROC}}(p) \xrightarrow{a.s.} \text{ROC}(p)$ . Moreover, the uniform convergence is obtained from the monotony of  $\widehat{\text{ROC}}$  and ROC and also from the continuity of ROC. ■

*Proof of Theorem 4.2.* From the monotony of  $\widehat{F}_j$  and  $F_j$  and also the continuity of  $F_j$ , it will be enough to prove that  $\widehat{F}_j(t) - F_j(t) \xrightarrow{a.s.} 0$ .

Fix  $j = D$  or  $H$ . Define  $\mathbb{L}_t^{(j)}(\boldsymbol{\beta}) = \mathbb{P}(\mathbf{x}_j^T \boldsymbol{\beta} \leq t)$  for any  $t \in \mathbb{R}$ , then

$$\left| \widehat{F}_j(t) - F_j(t) \right| \leq \left| \widehat{F}_{\widehat{\boldsymbol{\beta}},j}(t) - \mathbb{L}_t^{(j)}(\widehat{\boldsymbol{\beta}}) \right| + \left| \mathbb{L}_t^{(j)}(\widehat{\boldsymbol{\beta}}) - F_{\boldsymbol{\beta}_{0,j}}(t) \right| = \left| \widehat{F}_{\widehat{\boldsymbol{\beta}},j}(t) - F_{\widehat{\boldsymbol{\beta}},j}(t) \right| + \left| F_{\widehat{\boldsymbol{\beta}},j}(t) - F_{\boldsymbol{\beta}_{0,j}}(t) \right|.$$

It suffices to prove that

$$\sup_{t \in \mathbb{R}} \sup_{\boldsymbol{\beta} \in \mathbb{R}^k} \left| \widehat{F}_{\boldsymbol{\beta},j}(t) - F_{\boldsymbol{\beta},j}(t) \right| \xrightarrow{a.s.} 0 \quad (19)$$

and

$$\left| F_{\widehat{\boldsymbol{\beta}},j}(t) - F_{\boldsymbol{\beta}_0,j}(t) \right| \xrightarrow{a.s.} 0. \quad (20)$$

To derive (19), let us consider the family of functions

$$\mathcal{F} = \{h_{\boldsymbol{\beta},t}(\mathbf{x}) = \mathbb{I}_{\{\mathbf{x}^\top \boldsymbol{\beta} \leq t\}} \text{ for } (\boldsymbol{\beta}, t) \in \mathbb{R}^k \times \mathbb{R}\}.$$

Taking into account that  $\{g(\mathbf{x}) = \mathbf{x}^\top \boldsymbol{\beta} - t; (\boldsymbol{\beta}, t) \in \mathbb{R}^k \times \mathbb{R}\}$  is a finite-dimensional space of functions with dimension  $p+1$ , from Lemmas 9.6 in [Kosorok \(2008\)](#) we get that  $\mathcal{F}$  is a VC-class with index at most  $p+3$ . Hence, applying Lemmas 9.8 and 9.9(iii) in [Kosorok \(2008\)](#), we get that the class of functions  $\mathcal{F}$  is a VC-class with index  $V(\mathcal{F})$  smaller or equal than  $p+3$ . Note that the envelope of  $\mathcal{F}$  equals  $F \equiv 1$ . Hence, Theorem 2.6.7 in [van der Vaart and Wellner \(1996\)](#) entails that, there exists a universal constant  $K$  such that, for any measure  $Q$

$$N(\epsilon, \mathcal{F}, L_1(Q)) \leq K V(\mathcal{F}) (16e)^{V(\mathcal{F})} \left(\frac{1}{\epsilon}\right)^{V(\mathcal{F})-1},$$

which together with Theorem 2.4.3 in [van der Vaart and Wellner \(1996\)](#) or Theorem 2.4 in [Kosorok \(2008\)](#), leads to

$$\sup_{h \in \mathcal{F}} |P_{n_j} h - P_j h| \xrightarrow{a.s.} 0,$$

where we have used the standard notation in empirical processes, i.e.,  $P_h = \mathbb{E}h(\mathbf{X})$  and  $P_n h = (1/n) \sum_{i=1}^n h(\mathbf{x}_i)$ . Hence, we have that

$$\sup_{t \in \mathbb{R}} \sup_{\boldsymbol{\beta} \in \mathbb{R}^k} \left| \widehat{F}_{\boldsymbol{\beta},j}(t) - F_{\boldsymbol{\beta},j}(t) \right| \xrightarrow{a.s.} 0$$

which concludes the proof of (19).

It remains to prove (20). To strengthen the dependence on the sample size denote  $\widehat{\boldsymbol{\beta}}_n = \widehat{\boldsymbol{\beta}}$ , where  $n = n_D + n_H$ . Then, from the fact that  $\widehat{\boldsymbol{\beta}} \xrightarrow{a.s.} \boldsymbol{\beta}_0$ , there exists  $\mathcal{N} \subset \Omega$  such that  $\mathbb{P}(\mathcal{N}) = 0$  and for  $\omega \notin \mathcal{N}$ ,  $\widehat{\boldsymbol{\beta}}_n(\omega) \rightarrow \boldsymbol{\beta}_0$ . Take  $\omega \notin \mathcal{N}$ , then for any  $\mathbf{x} \in \mathbb{R}^k$ ,  $\mathbf{x}^\top \widehat{\boldsymbol{\beta}}_n(\omega) \rightarrow \mathbf{x}^\top \boldsymbol{\beta}_0$ . Hence, if  $\mathbf{x}_j \sim P_j$ , the random variable  $Z_n = \mathbf{x}_j^\top \widehat{\boldsymbol{\beta}}_n(\omega)$  converges to  $Z = \mathbf{x}_j^\top \boldsymbol{\beta}_0$  everywhere,

so  $F_{\widehat{\beta}_n(\omega),j}(t) = \mathbb{P}(Z_n \leq t) \rightarrow \mathbb{P}(Z \leq t) = F_j(t)$ , for any  $t$ . Using the fact that  $F_j(t)$  is non-decreasing and continuous, we conclude that, for any  $\omega \notin \mathcal{N}$ ,

$$\left\| F_{\widehat{\beta}_n(\omega),j} - F_j \right\|_{\infty} \rightarrow 0,$$

concluding the proof of (20). ■

*Proof of Theorem 4.3.* The proof is similar to that of Theorem 4.2. Denote  $\mathcal{H}_k$  the linear space spanned by  $\phi_1, \dots, \phi_k$ , that is,  $\mathcal{H}_k = \{\beta = \sum_{s=1}^k b_s \phi_s, \mathbf{b} = (b_1, \dots, b_k)^T \in \mathbb{R}^k\}$ .

Using that  $\widehat{F}_j$  and  $F_j$  are non-decreasing function and the continuity of  $F_j$ , it will be enough to show that  $\widehat{F}_j(t) - F_j(t) \xrightarrow{a.s.} 0$ . Fix  $j = D$  or  $H$  and define  $\mathbb{L}_t^{(j)}(\beta) = \mathbb{P}(\langle X_j, \beta \rangle \leq t)$ , then

$$\left| \widehat{F}_j(t) - F_j(t) \right| \leq \left| \widehat{F}_{\widehat{\beta},j}(t) - \mathbb{L}_t^{(j)}(\widehat{\beta}) \right| + \left| \mathbb{L}_t^{(j)}(\widehat{\beta}) - F_{\beta_0,j}(t) \right| = \left| \widehat{F}_{\widehat{\beta},j}(t) - \mathbb{L}_t^{(j)}(\widehat{\beta}) \right| + \left| F_{\widehat{\beta},j}(t) - F_{\beta_0,j}(t) \right|.$$

It is enough to show that

$$\sup_{t \in \mathbb{R}} \sup_{\beta \in \mathcal{H}_k} \left| \widehat{F}_{\beta,j}(t) - F_{\beta,j}(t) \right| \xrightarrow{a.s.} 0 \quad (21)$$

and

$$\left| F_{\widehat{\beta},j}(t) - F_{\beta_0,j}(t) \right| \xrightarrow{a.s.} 0. \quad (22)$$

The proof of (22) is similar to that of (20) and for that reason it is omitted.

To derive (21), we will follow similar arguments to those considered in the proof of Proposition 1 in Bianco and Boente (2023). Consider the family of functions

$$\mathcal{F} = \{h_{\beta,t}(x) = \mathbb{I}_{\{\langle x, \beta \rangle \leq t\}} \text{ for } (\beta, t) \in \mathcal{H}_k \times \mathbb{R}\}.$$

Taking into account that for  $\beta \in \mathcal{H}_k$ ,  $\langle x, \beta \rangle = \sum_{s=1}^k b_s \langle x, \phi_s \rangle = \mathbf{x}^T \mathbf{b}$ , where  $\mathbf{x} = (\langle x, \phi_1 \rangle, \dots, \langle x, \phi_k \rangle)^T$ , we obtain that  $\{g(x) = \langle x, \beta \rangle - t; (\beta, t) \in \mathcal{H}_k \times \mathbb{R}\}$  is a finite-dimensional space of functions with dimension  $k + 1$ . Thus, from Lemma 9.6 in Kosorok (2008) we get that  $\mathcal{F}$  is a VC-class with index at most  $k + 3$ . Hence, applying Lemmas 9.8 and 9.9(iii) in Kosorok (2008), we conclude that the class of functions  $\mathcal{F}$  is a VC-class with index  $V(\mathcal{F})$  smaller or equal than  $k + 3$ . Note that the envelope of  $\mathcal{F}$  equals  $F \equiv 1$ . Hence, Theorem 2.6.7 in van der Vaart and Wellner (1996) entails that, there exists a universal constant  $K$  such that, for any measure  $Q$

$$N(\epsilon, \mathcal{F}, L_1(Q)) \leq K (k + 3) (16e)^{k+3} \left( \frac{1}{\epsilon} \right)^{k+2}. \quad (23)$$

To show  $\sup_{h \in \mathcal{F}} |P_{n_j} h - P_j h| \xrightarrow{a.s.} 0$ , where  $P_j h = \mathbb{E}h(X_j)$  and  $P_{n_j} h = (1/n_j) \sum_{i=1}^{n_j} h(X_{j,i})$ , it will be enough to prove that

$$\frac{1}{n_j} \log N(\epsilon, \mathcal{F}, L_1(P_{n_j})) \xrightarrow{p} 0. \quad (24)$$

From (23) we get that

$$\frac{1}{n_j} \log N(\epsilon, \mathcal{F}, L_1(P_{n_j})) \leq C \frac{k+2}{n_j} \log \left( \frac{1}{\epsilon} \right),$$

for some constant  $C$ . Thus, using that  $k_n/n \rightarrow 0$ , we obtain that

$$\sup_{t \in \mathbb{R}} \sup_{\beta \in \mathcal{H}^k} \left| \widehat{F}_{\beta,j}(t) - F_{\beta,j}(t) \right| \xrightarrow{a.s.} 0.$$

which concludes the proof of (21). ■

*Proof of Theorem 4.4.* Note that b) is a direct consequence of a) and Theorem 4.1, so we will only show a). For that purpose recall that, for any  $\boldsymbol{\alpha} \in \mathbb{R}^k$  and  $\boldsymbol{\Lambda} \in \mathbb{R}^{k \times k}$ , we have denoted  $\Upsilon_{\boldsymbol{\Lambda}, \boldsymbol{\alpha}}(X) = -\mathbf{x}^T \boldsymbol{\Lambda} \mathbf{x} + \boldsymbol{\alpha}^T \mathbf{x}$  where  $\mathbf{x} = A(X) = (\langle X, \phi_1 \rangle, \dots, \langle X, \phi_k \rangle)^T$  and as in the proof of Theorem 4.3 let  $L_t^{(j)}(\boldsymbol{\Lambda}, \boldsymbol{\alpha}) = \mathbb{P}(\Upsilon_{\boldsymbol{\Lambda}, \boldsymbol{\alpha}}(X_j) \leq t)$ . Then,

$$|\widehat{F}_j(t) - F_j(t)| \leq |\widehat{F}_j(t) - L_t^{(j)}(\widehat{\boldsymbol{\Lambda}}, \widehat{\boldsymbol{\alpha}})| + |L_t^{(j)}(\widehat{\boldsymbol{\Lambda}}, \widehat{\boldsymbol{\alpha}}) - L_t^{(j)}(\boldsymbol{\Lambda}_0, \boldsymbol{\alpha}_0)|. \quad (25)$$

As in the proof of (20), the second term on the right hand side in (25) converges almost surely to 0, since  $(\widehat{\boldsymbol{\Lambda}}, \widehat{\boldsymbol{\alpha}}) \xrightarrow{a.s.} (\boldsymbol{\Lambda}_0, \boldsymbol{\alpha}_0)$ . Hence, we only have to show that  $\widehat{F}_j(t) - L_t^{(j)}(\widehat{\boldsymbol{\Lambda}}, \widehat{\boldsymbol{\alpha}}) \xrightarrow{a.s.} 0$ , which follows as in Theorem 4.2 using that the class of functions

$$\mathcal{F} = \left\{ h_{\boldsymbol{\Lambda}, \boldsymbol{\alpha}, t}(X) = \mathbb{I}_{\{-\mathbf{x}^T \boldsymbol{\Lambda} \mathbf{x} + \boldsymbol{\alpha}^T \mathbf{x} \leq t\}}, \boldsymbol{\Lambda} \in \mathbb{R}^{k \times k}, \boldsymbol{\alpha} \in \mathbb{R}^k, t \in \mathbb{R}, \text{ where } \mathbf{x} = A(X) \right\},$$

is a finite-dimensional space of functions. ■

## References

- Bali, J. L. and Boente, G. (2009). Principal points and elliptical distributions from the multivariate setting to the functional case. *Statistics and Probability Letters*, 79:1858–1865.
- Benko, M. and Härdle, W. (2005). Common functional implied volatility analysis. *In Statistical Tools for Finance and Insurance, Eds: Pavel Čížek, Rafal Weron and Wolfgang Härdle*, pages 115–134. Springer.

- Bianco, A. M. and Boente, G. (2023). Addressing robust estimation in covariate-specific ROC curves. *Econometrics and Statistics*. In press, available at <https://doi.org/10.1016/j.ecosta.2023.04.001>.
- Boente, G., Rodríguez, D., and Sued, M. (2010). Inference under functional proportional and common principal components models. *Journal of Multivariate Analysis*, 101:464–475.
- Boente, G., Salibián-Barrera, M., and Tyler, D. (2014). A characterization of elliptical distributions and some optimality properties of principal components for functional data. *Journal of Multivariate Analysis*, 131:254–264.
- Coffey, N., Harrison, A. J., Donaghue, O. A., and Hayes, K. (2011). Common functional principal components analysis: A new approach to analyzing human movement data. *Human Movement Science*, 30:1144–1166.
- Estévez-Pérez, G. and Vieu, P. (2021). A new way for ranking functional data with applications in diagnostic test. *Computational Statistics*, 36:127–154.
- Ferraty, F. and Vieu, P. (2006). *Nonparametric Functional Data Analysis: Theory and Practice*. Springer.
- Flury, B. (1984). Common principal components in  $k$  groups. *Journal of the American Statistical Association*, 79:892–898.
- Flury, B. (1988). *Common Principal Components and Related Multivariate Models*. Wiley.
- Flury, B. and Schmid, M. (1992). Quadratic discriminant functions with constraints on the covariances matrices: Some asymptotic resultss. *Journal of Multivariate Analysis*, 40:244–261.
- Frahm, G. (2004). *Generalized Elliptical Distributions: Theory and Applications*. PhD thesis, University of Köln, Germany.
- Haben, M., Tian, L., and Ghebremichael, M. (2019). The ROC curve for regularly measured longitudinal biomarkers. *Biostatistics*, 20:433–451.
- He, G., Müller, H., Wang, J., and Yang, W. (2003). Functional canonical analysis for square integrable stochastic processes. *Journal of Multivariate Analysis*, 85:54–77.
- Horváth, L. and Kokoszka, P. (2012). *Inference for Functional Data with Applications*. Springer.

- Hsing, T. and Eubank, R. (2015). *Theoretical foundations of Functional Data Analysis with an introduction to Linear Operators*, volume 997. John Wiley and Sons.
- Hult, H. and Lindskog, F. (2002). Multivariate extremes, aggregation and dependence in elliptical distributions. *Advances in Applied Probability*, 34:587–608.
- Inácio, V., González-Manteiga, W., Febrero-Bande, M., Gude, F., Alonzo, T., and Cadarso-Suárez, C. (2012). Extending induced ROC methodology to the functional context. *Biostatistics*, 13:594–608.
- Inácio de Carvalho, V., de Carvalho, M., Alonzo, T., and González-Manteiga, W. (2016). Functional covariate-adjusted partial area under the specificity-ROC curve with an application to metabolic syndrome diagnosis. *Annals of Applied Statistics*, 10:1472–1495.
- Jang, J. H. and Mantunga, A. (2022). Diagnostic evaluation of pharmacokinetic features of functional markers. *Journal of Biopharmaceutical Statistics*, 33:307–323.
- Kosorok, M. R. (2008). *Introduction to Empirical Processes and Semiparametric Inference*. Springer.
- Krzanowski, W. J. and Hand, D. J. (2009). *ROC Curves for Continuous Data*. Chapman and Hall.
- Leurgans, S. E., Moyeed, R. A., and Silverman, B. W. (1993). Canonical correlation analysis when the data are curves. *Journal of the Royal Society, Series B*, 55:725–740.
- Liu, H., Li, G., Cumberland, W., and Wu, T. (2005). Testing statistical significance of the area under a receiving operating characteristics curve for repeated measures design with bootstrapping. *Journal of Data Science*, 3:257–278.
- Liu, H. and Wu, T. (2003). Estimating the area under a receiver operating characteristic (ROC) curve for repeated measures design. *Journal of Statistical Software*, 8:1–18.
- Ma, S. and Huang, J. (2005). Regularized ROC method for disease classification and biomarker selection with microarray data. *Bioinformatics*, 21:4356–4362.
- Ma, S. and Huang, J. (2007). Combining multiple markers for classification using ROC. *Biometrics*, 63:751–757.
- Pepe, M. (2003). *The Statistical Evaluation of Medical Tests for Classification and Prediction*. Oxford University Press.

- Pepe, M., Cai, T., and Longton, G. (2006). Combining predictors for classification using the area under the Receiver Operating Characteristic Curve. *Biometrics*, 62:221–229.
- Pérez-Fernández, S. (2020). *ROC curves for multivariate markers*. PhD thesis, PhD. dissertation, Universidad de Oviedo and Technische Universität Wien (supervisors Corral Blanco, N., Martínez Camblor, P. and Filzmoser, P.).
- Piñeiro-Lamas, B., López-Cheda, A., Cao, R., Ramos-Alonso, L., González-Barbeito, G., Barbeito-Caamaño, C., and Bouzas-Mosquera, A. (2023). A cardiotoxicity dataset for breast cancer patients. *Scientific Data*, 10:527.
- Ramsay, J. and Silverman, B. (2005). *Functional Data Analysis, 2nd edition*. Springer.
- Sun, Y. and Genton, M. G. (2011). Functional boxplots. *Journal of Computational and Graphical Statistics*, 20:316–334.
- van der Vaart, A. W. and Wellner, J. A. (1996). *Weak Convergence and Empirical Processes*. Springer, New York.
- Wang, J. L., Chiou, J., and Müller, H. (2016). Functional data analysis. *Annual Review of Statistics and Its Application*, 3:257–295.
- Zhou, X. H., McClish, D. K., and Obuchowski, N. A. (2011). *Statistical Methods in Diagnostic Medicine*. John Wiley & Sons, New York.